



**HAL**  
open science

# **MT5-MMP promotes neuroinflammation, neuronal excitability and $A\beta$ production in primary neuron/astrocyte cultures from the 5xFAD mouse model of Alzheimer's disease**

Dominika Pilat, Jean-Michel Paumier, Laura García-González, Laurence Louis, Delphine Stephan, Christine Manrique, Michel Khrestchatisky, Eric Di Pasquale, Kévin Baranger, Santiago Rivera

## **► To cite this version:**

Dominika Pilat, Jean-Michel Paumier, Laura García-González, Laurence Louis, Delphine Stephan, et al.. MT5-MMP promotes neuroinflammation, neuronal excitability and  $A\beta$  production in primary neuron/astrocyte cultures from the 5xFAD mouse model of Alzheimer's disease. *Journal of Neuroinflammation*, In press, 10.1186/s12974-022-02407-z . hal-03570912

**HAL Id: hal-03570912**

**<https://hal.science/hal-03570912>**

Submitted on 13 Feb 2022

**HAL** is a multi-disciplinary open access archive for the deposit and dissemination of scientific research documents, whether they are published or not. The documents may come from teaching and research institutions in France or abroad, or from public or private research centers.

L'archive ouverte pluridisciplinaire **HAL**, est destinée au dépôt et à la diffusion de documents scientifiques de niveau recherche, publiés ou non, émanant des établissements d'enseignement et de recherche français ou étrangers, des laboratoires publics ou privés.

RESEARCH

Open Access



# MT5-MMP promotes neuroinflammation, neuronal excitability and A $\beta$ production in primary neuron/astrocyte cultures from the 5xFAD mouse model of Alzheimer's disease

Dominika Pilat<sup>1†</sup>, Jean-Michel Paumier<sup>1,2†</sup>, Laura García-González<sup>1,3</sup>, Laurence Louis<sup>1</sup>, Delphine Stephan<sup>1</sup>, Christine Manrique<sup>1</sup>, Michel Khrestchatisky<sup>1</sup>, Eric Di Pasquale<sup>1</sup>, Kévin Baranger<sup>1\*</sup> and Santiago Rivera<sup>1\*</sup>

## Abstract

**Background:** Membrane-type matrix metalloproteinase 5 (MT5-MMP) deficiency in the 5xFAD mouse model of Alzheimer's disease (AD) reduces brain neuroinflammation and amyloidosis, and prevents deficits in synaptic activity and cognition in prodromal stages of the disease. In addition, MT5-MMP deficiency prevents interleukin-1 beta (IL-1 $\beta$ )-mediated inflammation in the peripheral nervous system. In this context, we hypothesized that the MT5-MMP/IL-1 $\beta$  tandem could regulate nascent AD pathogenic events in developing neural cells shortly after the onset of transgene activation.

**Methods:** To test this hypothesis, we used 11–14 day in vitro primary cortical cultures from wild type, MT5-MMP<sup>-/-</sup>, 5xFAD and 5xFAD/MT5-MMP<sup>-/-</sup> mice, and evaluated the impact of MT5-MMP deficiency and IL-1 $\beta$  treatment for 24 h, by performing whole cell patch-clamp recordings, RT-qPCR, western blot, gel zymography, ELISA, immunocytochemistry and adeno-associated virus (AAV)-mediated transduction.

**Results:** 5xFAD cells showed higher levels of MT5-MMP than wild type, concomitant with higher basal levels of inflammatory mediators. Moreover, MT5-MMP-deficient cultures had strong decrease of the inflammatory response to IL-1 $\beta$ , as well as decreased stability of recombinant IL-1 $\beta$ . The levels of amyloid beta peptide (A $\beta$ ) were similar in 5xFAD and wild-type cultures, and IL-1 $\beta$  treatment did not affect A $\beta$  levels. Instead, the absence of MT5-MMP significantly reduced A $\beta$  by more than 40% while sparing APP metabolism, suggesting altogether no functional crosstalk between IL-1 $\beta$  and APP/A $\beta$ , as well as independent control of their levels by MT5-MMP. The lack of MT5-MMP strongly down-regulated the AAV-induced neuronal accumulation of the C-terminal APP fragment, C99, and subsequently that of A $\beta$ . Finally, MT5-MMP deficiency prevented basal hyperexcitability observed in 5xFAD neurons, but not hyperexcitability induced by IL-1 $\beta$  treatment.

\*Correspondence: kevin.baranger@univ-amu.fr; santiago.rivera@univ-amu.fr

<sup>†</sup>Dominika Pilat and Jean-Michel Paumier equally contributed to this work

<sup>1</sup> Institute of Neuropathophysiology (INP), UMR 7051, Aix-Marseille Univ, CNRS, Campus Santé Timone, 27 Bld Jean Moulin, 13005 Marseille, France

Full list of author information is available at the end of the article



© The Author(s) 2022. **Open Access** This article is licensed under a Creative Commons Attribution 4.0 International License, which permits use, sharing, adaptation, distribution and reproduction in any medium or format, as long as you give appropriate credit to the original author(s) and the source, provide a link to the Creative Commons licence, and indicate if changes were made. The images or other third party material in this article are included in the article's Creative Commons licence, unless indicated otherwise in a credit line to the material. If material is not included in the article's Creative Commons licence and your intended use is not permitted by statutory regulation or exceeds the permitted use, you will need to obtain permission directly from the copyright holder. To view a copy of this licence, visit <http://creativecommons.org/licenses/by/4.0/>. The Creative Commons Public Domain Dedication waiver (<http://creativecommons.org/publicdomain/zero/1.0/>) applies to the data made available in this article, unless otherwise stated in a credit line to the data.



Journal : **BMCTwo 12974**

Dispatch : **3-2-2022**

Pages : **21**

Article No : **2407**

LE

TYPESET

MS Code :

CP

DISK

**Conclusions:** Neuroinflammation and hyperexcitability precede A $\beta$  accumulation in developing neural cells with nascent expression of AD transgenes. MT5-MMP deletion is able to tune down basal neuronal inflammation and hyperexcitability, as well as APP/A $\beta$  metabolism. In addition, MT5-MMP deficiency prevents IL-1 $\beta$ -mediated effects in brain cells, except hyperexcitability. Overall, this work reinforces the idea that MT5-MMP is at the crossroads of pathogenic AD pathways that are already incipiently activated in developing neural cells, and that targeting MT5-MMP opens interesting therapeutic prospects.

**Keywords:** Neuroinflammation, IL-1 $\beta$ , Amyloid peptide, Amyloid precursor protein, C99, Synaptic activity, Matrix metalloproteinase, Neuroprotection, AAV, Patch-clamp

## Background

Membrane-type matrix metalloproteinase 5 (MT5-MMP; also known as MMP-24) is a member of the matrix metalloproteinase (MMP) family of Zn<sup>2+</sup>-dependent pleiotropic endopeptidases [1]. MT5-MMP is the only MMP preferentially expressed in the nervous system [2] and is involved in different forms of neural cell plasticity (reviewed in [3, 4]) that include axonal outgrowth [5], post-lesion axonal sprouting [6], and neural stem cell differentiation of precursor cells expressing glial fibrillary acidic protein (GFAP) [7]. Only a handful of MT5-MMP interacting proteins or substrates have been identified, providing potential queues for the interpretation of MT5-MMP functions. Thus, MT5-MMP interacts with the AMPA receptor binding protein (ABP) and the glutamate receptor-interacting protein (GRIP) [8], both hosting PDZ domains that drive AMPA receptor targeting to the plasma membrane. MT5-MMP also cleaves E- and N-cadherins [7–10], involved in synapse organization and stability. Amyloid precursor protein (APP) is another relevant substrate of MT5-MMP [11–13], which holds a central position in Alzheimer's disease (AD) pathogenesis. APP processing by  $\alpha$ - and  $\beta$ -secretase generates C-terminal fragments (CTF) known as C83 and C99, respectively. Further intramembrane processing of C99 by  $\gamma$ -secretase releases the amyloid beta peptide (A $\beta$ ). Accumulation of C99 and A $\beta$  is a hallmark of the pathogenic amyloidogenic cascade in Alzheimer's disease (AD) [14], while C83 is the major physiological APP fragment generated by human [15] and murine [16] neurons. Alternative to canonical APP processing, MT5-MMP has been shown to cleave APP and to generate a  $\eta$ -CTF from which subsequent processing by  $\alpha$ -secretase releases an A $\eta$ - $\alpha$  fragment that inhibits LTP in cellulo [12]. We found this cleavage to occur in vivo in the brains of the 5xFAD mouse model of AD [13]. MT5-MMP is a new pro-amyloidogenic factor, whose deficiency markedly reduced the levels of A $\beta$  and C99 in early stages of the pathology, concomitant with prevention of deficits in long-term potentiation (LTP), spatial learning and working memory [13, 17]. MT5-MMP deficiency also prevented glial reactivity and the increase in the levels of pro-inflammatory

interleukin-1 beta (IL-1 $\beta$ ) [13] in 5xFAD mice. IL-1 $\beta$  is a major neuroinflammatory mediator, highly expressed in AD following activation of the NLRP3 inflammasome [18–20], and shows complex and diverse effects on neurons including disruption of synaptic plasticity [21], promotion of excitotoxicity [22, 23] and  $\alpha$ - and  $\gamma$ -secretase activities, while reducing  $\beta$ -secretase activity [24, 25] and A $\beta$  levels [26, 27]. Interestingly, IL-1 $\beta$  failed to induce the expected neuroinflammation after injection into the paws of MT5-MMP-deficient mice in a model of thermal pain, unveiling functional interactions between MT5-MMP and IL-1 $\beta$  in the peripheral nervous system (PNS) through a mechanism involving N-cadherin [10].

Together, these data extend the scope of MT5-MMP actions beyond APP processing, as previously suggested [28] and led us to hypothesize that MT5-MMP modulates, possibly in concert with IL-1 $\beta$ , three major events in AD: APP/A $\beta$  metabolism, neuroinflammation, and neuronal activity. It was also our objective to explore the possibility that such modulations occur in young neural cells of 5xFAD brains, well before the first pathological signs. We tested these hypotheses using mixed neuron/astrocyte primary cortical cultures from wild type (WT), 5xFAD (Tg), MT5-MMP<sup>-/-</sup> (MT5<sup>-/-</sup>) and 5xFAD/MT5-MMP<sup>-/-</sup> (TgMT5<sup>-/-</sup>) mice [13, 17] stimulated or not by IL-1 $\beta$ . Our study reveals that MT5-MMP modulates A $\beta$  and C99, IL-1 $\beta$ -mediated inflammation, and synaptic activity in young neurons, overall highlighting a key role for this proteinase in early molecular and cellular events that may preconfigure AD pathology.

## Materials and methods

### Mixed neuronal glial cultures and treatments

To generate mixed neuronal–glial cell cultures, we used WT, MT5<sup>-/-</sup>, Tg and TgMT5<sup>-/-</sup> mice in a C57BL6 genetic background as previously described [13, 17]. All the experimental procedures were conducted in agreement with the authorization for animal experimentation attributed by the French Ministry of Research to the laboratory (research project: APAFIS#23040-2019112708474721 v4). Briefly, pregnant females were deeply anesthetized with xylazine



(15 mg/kg) and ketamine (150 mg/kg) (Ceva Santé animale, Libourne, France), and E16 embryos extracted from the uterine horns and cerebral cortices were dissected. All the culture media, fetal bovine serum (FBS), reagents and supplements for cell culture were purchased from ThermoFisher Scientific (Villebon-sur-Yvette, France). Cortices were placed into cold HBSS1X medium and dissociated for 10 min at 37 °C in HBSS1X containing DNase I (10 µg/mL) and 0.1% trypsin. Reaction was stopped by the addition of a DMEM solution containing 10% FBS and further mechanical dissociation was performed through a pipette cone. After centrifugation for 5 min at 300×g, 3.10<sup>5</sup> cells/well were plated onto 6-well plates pre-coated with poly-L-lysine (10 µg/mL, Sigma-Aldrich, Saint-Quentin Fallavier, France) for 2 h in DMEM medium containing 10% FBS and 1% penicillin/streptomycin (P/S). This medium was further replaced by Neurobasal containing B27, 1% glutamine and 1% P/S for 11 days in vitro (DIV) without anti-mitotic agent. Cells were treated or not with IL-1β (10 ng/mL, Pepro-Tech, Neuilly-sur-Seine, France) and/or DAPT (10 µM, Tocris, Bio-Techne, Lille, France) or proteasome inhibitor MG132 (5 µM, Enzo Life Science, Lyon, France), 24 h before collection in either RIPA buffer (Sigma-Aldrich) for western blot (WB) analyses or collected for RNA extraction. For ICC experiments, cells were plated at 1.10<sup>5</sup> density on 24-well plates on coverslips pre-coated with 500 µg/mL of poly-L-lysine. For electrophysiological experiments, cells were plated as described above for ICC and recorded between 11 and 14 DIV.

#### MTT test

Cell viability was evaluated using the 3-(4,5-dimethylthiazol-2-yl)-2,5-diphenyl tetrazolium bromide (MTT) assay (Sigma-Aldrich), which measures mitochondrial activity in living cells. A solution at 5 mg/mL was prepared into Neurobasal and then added to cultures at a final concentration 0.5 mg/mL for 3 h at 37 °C, 5% CO<sub>2</sub>. Media were fully removed and 200 µL of DMSO added, then 100 µL of DMSO were transferred into a 96-well plate and absorbance (OD) at 550 nm was read in a spectrophotometer. Data were calculated as the percentage of living cells = (transfected cell OD<sub>550</sub>/control cell OD<sub>550</sub>) × 100. The mean values ± SEM were obtained from at least five animals by genotype.

#### Viral infections

An empty AAV10 or encoding human C99 under control of the synapsin-1 promoter (AAV-empty or AAV-C99 thereafter) were previously described [29] and kindly provided by Dr. Raphaëlle Pardossi-Piquard. WT and MT5<sup>-/-</sup> neurons were transduced at 6 DIV with 2 µL (at

5.10<sup>12</sup> vg/mL, MOI = 2.5 × 10<sup>4</sup>), treated at 10 DIV with DAPT (10 µM) and recovered at 11 DIV for WB analyses.

#### Western blot

Protein concentration was determined using a Bio-Rad DC™ protein assay kit (Bio-Rad, Marnes-La-Coquette, France). Proteins (30 µg) were loaded and run on 10–15% SDS-PAGE gels, or 4–20% Tris–Glycine pre-casted gels or low molecular weight 16% Tris–Tricine pre-casted gels (ThermoFisher Scientific) and transferred onto nitrocellulose membranes (Dutscher, Brumath, France). After blocking, membranes were probed with the following antibodies directed against MT5-MMP (1/500, our own antibody previously described [13]), or APP N-terminal fragment (22C11, 1/1000, Millipore, Merck Millipore, Molsheim, France), APP C-terminal fragment (APP-CTF, 1/1000, Sigma-Aldrich), human Aβ (6E10, 1/500, Ozyme, Saint-Cyr l'École, France), Aβ/C99 (82E1, 1/100, IBL America, Illkirch-Graffenstaden, France), GFAP (1/1000, Millipore), IL-1β (1/500, PeproTech), N-cadherin (1/1000, BD Biosciences, Le Pont de Claix, France), MAP-2 (1/500, Sigma-Aldrich), β-III tubulin (1/1000, Sigma-Aldrich), LRP-1 (1/1000, Abcam, Cambridge, United Kingdom), RAGE (1/1000, Abcam), LDLR (1/1000, Proteintech Europe, Manchester, United Kingdom), LRP-8 (1/250, Abcam), Histone 3 (1/1000, Abcam), Na<sup>+</sup>/K<sup>+</sup> ATPase (1/1000, Abcam), β-actin (1/5000, Sigma-Aldrich), GAPDH (1/5000, Sigma-Aldrich), and then incubated with horseradish peroxidase-conjugated secondary IgG antibodies (Jackson ImmunoResearch, Interchim, Montluçon, France). Note that depending on the molecular weight of the proteins studied and thus the gels used, GAPDH, β-actin or ponceau S staining of the membrane [30, 31] were used as loading and normalization controls. Immunoblot signals were visualized using the ECL chemiluminescence kit (Dutscher) and quantified using Fiji/Image J software (NIH). Note that immunoblots were represented in separated columns when bands from the same membrane were not adjacent.

#### Subcellular fractionation

Cytoplasmic, membranous, and nuclear fractions were prepared from cell lysates using a ProteoExtract® Subcellular Proteome Extraction Kit (Calbiochem, Merck Millipore, Molsheim, France) according to the manufacturer's instructions. The purity of each fraction was analyzed by western blot, as described above using antibodies against GAPDH, Na<sup>+</sup>/K<sup>+</sup> ATPase and Histone 3 for cytoplasmic, membranous and nuclear fractions, respectively.

#### Gel zymography

We used gelatin zymography on culture supernatants to assess changes in the levels of MMP-2 and MMP-9, also



220 known as gelatinase A and B, respectively. As previously  
221 described [32], equal amounts of serum-free superna-  
222 tants in non-denaturing and non-reducing conditions  
223 were subjected to zymography according to the manufac-  
224 turer's recommendations (ThermoFisher Scientific). Gels  
225 were scanned using GeneTools software.

#### 226 Reverse transcription-quantitative polymerase chain 227 reaction (RT-qPCR)

228 Total RNA was extracted from 11 DIV cells using the  
229 Nucleospin RNA kit (Macherey–Nagel, Hoerd, France)  
230 according to the manufacturer's recommendations. All  
231 the reagents for RT-qPCR experiments were purchased  
232 from ThermoFisher Scientific. Single-stranded cDNA  
233 was synthesized from 500 ng of RNA using the High-  
234 Capacity RNA to cDNA™ kit adapted for quantitative  
235 PCR. Twenty-five ng of cDNA were subjected to a qPCR  
236 reaction using the Fast Real-Time PCR System. For each  
237 experiment, cDNA samples were analyzed in duplicate  
238 and relative gene expression was obtained using the  
239 comparative  $2^{-\Delta\Delta C_t}$  method after normalization to the  
240 *Gapdh* (Mm99999915\_g1) housekeeping gene [32, 33].  
241 The expression of the following genes was measured:  
242 *Mmp24* (Mm00487721\_m1), *Mmp14* (Mm00485054\_  
243 m1), *Il-1 $\beta$*  (Mm01336189\_m1), *Gfap* (Mm01253033\_m1),  
244 *Ccl2* (Mm00441242\_m1), *Mmp2* (Mm00439498\_m1),  
245 *Mmp9* (Mm00442991\_m1), *Ide* (Mm00473077\_m1),  
246 *Ace* (Mm00802048\_m1), *Ece* (Mm01187091\_m1), *Tnfr*  
247 (Mm00443258\_m1), *Bace1* (Mm00478664\_m1), *Psen1*  
248 (Mm00501184\_m1), *Adam10* (Mm00545742\_m1),  
249 *Lrp1* (Mm0046458\_m1), *Lrp8* (Mm00474023\_m1), *Ldlr*  
250 (Mm00440169\_m1), *Ager* (Mm00545815\_m1), *APP*  
251 (Hs00169098\_m1), *PSEN1* (Hs00997789\_m1).

#### 252 Immunocytochemistry

253 After 11 DIV, our neural cultures were fixed for 15 min  
254 with AntigenFix (Diapath, MM France, Brignais, France)  
255 and blocked with PBS1X, BSA 3%, 0.1% Triton X-100  
256 (blocking solution) for 1 h. Primary antibodies GFAP  
257 (Dako France, Trappes, France), Iba1 (Wako, Sobi-  
258 oda, Mont-Bonnot Saint-Martin, France),  $\beta$ -III tubulin  
259 (Sigma-Aldrich), were used at 1/500 dilution. Approp-  
260 iate AlexaFluor-coupled secondary antibodies were used  
261 at 1/800 dilution. Hoechst 33,342 (0.5  $\mu$ g/mL) was used  
262 to stain the nuclei. Antibodies and Hoechst were diluted in  
263 blocking solution. Omission of the primary antibody was  
264 used as control and no immunostaining was observed.  
265 Samples were mounted using Prolong Gold Antifading  
266 reagent on Superfrost glass slides (Dutscher). Images  
267 were taken and processed using a confocal microscope  
268 (LSM 700) and Zen software (Zeiss, Jena, Germany).

#### ELISA

269 Total A $\beta$ 38, A $\beta$ 40 and A $\beta$ 42 levels in culture superna-  
270 tants were assessed by ELISA using the V-PLEX Plus A $\beta$   
271 Peptide Panel 1 (4G8) Kit (Meso Scale Discovery, Rock-  
272 ville, Maryland, USA) according to the manufacturer's  
273 recommendations. The MSD kit uses 4G8 as a capture  
274 antibody that recognizes both mouse and human A $\beta$ .  
275 Specific A $\beta$ 38, A $\beta$ 40 and A $\beta$ 42 were used for detec-  
276 tion. Therefore, the measured A $\beta$  levels are a mixture of  
277 endogenous mouse A $\beta$  and human A $\beta$  derived from the  
278 processing of human APP. Human A $\beta$ 40 levels in culture  
279 supernatants after AAV-C99 infections were evaluated  
280 using the human A $\beta$ 40 ELISA kit (#KHB3481, Ther-  
281 moFisher Scientific). For detection of IL-1 $\beta$  and MCP-1  
282 in supernatants, we used the murine IL-1 $\beta$  and MCP-1  
283 ELISA Development Kits (PeproTech). IL-6 protein lev-  
284 els were measured using V-PLEX Proinflammatory  
285 Panel 1 mouse Kit (K15048D-1, Meso Scale Discovery,  
286 Rockville, Maryland, USA). Analyses were done using a  
287 QuickPlex SQ 120 instrument (MSD) and DISCOVERY  
288 WORKBENCH® 4.0 software. All these assays were used  
289 as recommended by the manufacturers. 290

#### Electrophysiology

##### Patch-clamp

291 Whole-cell recordings were performed on neurons with  
292 pyramidal shape using an Axopatch200B amplifier (Axon  
293 Instruments, Axon Digidata 1550, Molecular Device, San  
294 José, California) under visual control, using a Zeiss Exam-  
295 iner A1 infraRed differential interference contrast micro-  
296 scope (Zeiss Mediatech, Marly le Roi, France) coupled to a  
297 Jenoptik ProgRes MF camera (Carl Zeiss, Jena, Germany).  
298 Patch microelectrodes (1.5 mm OD, borosilicate filament  
299 glass, BF150 from WPI) were pulled using a PP-830 elec-  
300 trode puller (Narishige, Fulbourn, Cambridge, UK), filled  
301 with 100 mM CsCl, 30 mM CsF, 10 mM N-2-hydroxy-  
302 ethylpiperazine-N-2-ethanesulphonic acid (HEPES),  
303 5 mM ethylene glycol-bis (b-aminoethylether)-N,N,N',  
304 N-tetraacetic acid (EGTA), and 1 mM MgCl<sub>2</sub>. Two mM  
305 CaCl<sub>2</sub> and 4 mM Mg-ATP/0.4 mM Na<sub>2</sub>-GTP was added  
306 on the day of the experiment (pH 7.4, balanced with  
307 CsOH). Pipettes (4–6 M $\Omega$ ) were directed onto neurons  
308 using a motorized Sutter microdrive (ROE200, Sutter  
309 Instrument Co WPI, Friedberg, Germany). The offset  
310 between the reference electrode and the patch pipette  
311 was zeroed upon contact of the recording chamber extra-  
312 cellular medium (aCSF, artificial Cerebro-Spinal Fluid  
313 140 mM NaCl, 3 mM KCl, 10 mM Hepes, 10 mM glu-  
314 cose, 2.5 mM CaCl<sub>2</sub>, 1 mM MgCl<sub>2</sub>, 300 nM TTX, pH 7.4  
315 with NaOH). The reference electrode was an Ag–AgCl  
316 wire connected to the extracellular solution. Selected  
317 pyramidal neurons had gigaohm seals (typically 1–5  
318 319



320 G $\Omega$ ), a stable resting membrane potential and an access  
321 resistance < 15 M $\Omega$  that was not compensated for.

### 322 **Recording and analysis of baseline synaptic transmission**

323 In voltage-clamp mode, cells were held at -50 mV and  
324 miniature global post-synaptic currents (gPSCs) were  
325 recorded for 5 min (band width, 1 kHz), after a 5-min  
326 recovery from breaking through the plasma membrane.  
327 We did not make any distinction between excitatory or  
328 inhibitory synaptic currents. The analysis was run offline  
329 using the Clampfit11 (Axon Instruments) routines.  
330 gPSCs were selected individually for each neuron of each  
331 genotype and pharmacological condition. Statistics were  
332 then obtained regarding the mean amplitude and the  
333 mean frequency of gPSCs occurrence during 5 min to  
334 generate the histograms.

### 335 **Statistics**

336 All values represent the means  $\pm$  SEM of the number of  
337 independent cultures indicated in the figure legends. For  
338 statistical analyses, we used ANOVA followed by a Fisher's  
339 LSD post hoc test and set the statistical significance  
340 at  $p < 0.05$ . Analyses were performed with the GraphPad  
341 Prism software (San Diego, California USA).

## 342 **Results**

### 343 **Neural 5xFAD cells show upregulation of MT5-MMP, but its 344 deficiency and IL-1 $\beta$ treatment do not impact cell stability**

345 As expected, neuron/astrocyte cultures from MT5<sup>-/-</sup>  
346 mice did not express *Mmp24* mRNA, which encodes  
347 MT5-MMP (Fig. 1A). In addition, there was no difference  
348 in *Mmp24* mRNA levels between WT and Tg cells, even  
349 after IL-1 $\beta$  treatment (10 ng/mL) (Fig. 1A). We confirmed  
350 the depletion of MT5-MMP protein in our cells (Fig. 1B)  
351 and also found a 76% increase of MT5-MMP levels in Tg  
352 cells compared to WT that was maintained under IL-1 $\beta$   
353 (Fig. 1B). *Mmp14* (MT1-MMP) is a close homolog of  
354 *Mmp24* (MT5-MMP) which shares pro-amyloidogenic  
355 features [33, 34]. Accordingly, tested for possible compensatory  
356 effects, but *Mmp14* mRNA remained stable  
357 in all genotypes and thus did not compensate for MT5-  
358 MMP deficiency, regardless of IL-1 $\beta$  treatment (Fig. 1C).

359 Cultures were roughly estimated at 2/3 of neurons  
360 ( $\beta$ -III tubulin<sup>+</sup>) and 1/3 of astrocytes (GFAP<sup>+</sup>), while no  
361 microglia was detected (Iba1<sup>+</sup>). A representative image of  
362 WT neural cells, treated or not with IL-1 $\beta$ , is shown in  
363 Fig. 1D. Moreover, levels of the  $\beta$ -III tubulin (Fig. 1E) and  
364 MAP-2 (not shown) neuronal markers were stable across  
365 genotypes in all experimental conditions, as revealed by  
366 WB. Likewise, there was no change in the content of the  
367 astrocytic marker GFAP (Fig. 1F). Moreover, the MTT  
368 test confirmed no cytotoxic effects associated with geno-  
369 types or IL-1 $\beta$  treatment in our conditions (Fig. 1G).

### 370 **The expression of genes coding for inflammatory 371 mediators is selectively altered in MT5-MMP-deficient cells**

372 As previously shown in the peripheral nervous system,  
373 MT5-MMP deficiency appeared to interfere with IL-1 $\beta$ -  
374 mediated response [10]. Accordingly, we questioned  
375 whether this might also be the case in the central nervous  
376 system (CNS). We first analyzed the effect of genotype  
377 on basal levels of key AD inflammatory mediators and  
378 found that IL-1 $\beta$  mRNA was drastically decreased by 77%  
379 in TgMT5<sup>-/-</sup> cells compared with Tg (Fig. 2A). Similarly,  
380 *Ccl2* mRNA, which encodes monocyte chemoattractant  
381 protein-1 (MCP-1) (Fig. 2B) and *Il-6* mRNA were both  
382 significantly decreased by 63% and 52% in TgMT5<sup>-/-</sup>  
383 cells, compared with Tg, respectively (Fig. 2C). Only *Tnfa*  
384 (TNF- $\alpha$ ) expression remained selectively unchanged  
385 between genotypes (Fig. 2D).

386 IL-1 $\beta$  is a key cytokine in AD [20] that stimulates its  
387 own expression [35, 36] as well as that of other inflam-  
388 matory mediators, including *Il-6*, *Ccl2* and *Tnfa* [37–40].  
389 In pace with these data, IL-1 $\beta$  induced its own mRNA  
390 in WT (174%) and Tg (109%) cultures (Fig. 2E), but not  
391 in cells lacking MT5-MMP (MT5<sup>-/-</sup> and TgMT5<sup>-/-</sup>)  
392 (Fig. 2E). *Ccl2* mRNA levels, which were relatively low  
393 in basal conditions, respectively reached 5000% and  
394 4000% increases in WT and Tg cells after IL-1 $\beta$  exposure  
395 (Fig. 2F). Again, the stimulating effect of IL-1 $\beta$  on *Ccl2*  
396 was hampered by MT5-MMP deficiency, with mRNA  
397 levels significantly reduced by 55% and 49% in MT5<sup>-/-</sup>  
398 and TgMT5<sup>-/-</sup> cells compared with their respective WT  
399 and Tg controls. IL-1 $\beta$  treatment upregulated *Il-6* levels

(See figure on next page.)

**Fig. 1** Effects of MT5-MMP deficiency and IL-1 $\beta$  treatment on primary cultures of cortical neural cells. **A** mRNA levels of *Mmp24* analyzed by RT-qPCR. Data values were normalized by *Gapdh* as housekeeping gene. **B** MT5-MMP levels detected by immunoblot (top panel) with its corresponding quantification (lower panel) normalized with  $\beta$ -actin. Note that MT5-MMP was not detected in MT5<sup>-/-</sup> and TgMT5<sup>-/-</sup> cells. **C** mRNA levels of *Mmp14* analyzed by RT-qPCR. Data values were normalized by *Gapdh* as housekeeping gene. **D** Representative confocal micrographs of primary neuronal cultures from WT mice treated or not with IL-1 $\beta$  and labeled with astrocytic marker GFAP (green) and neuronal marker  $\beta$ -III tubulin (red). Nuclei are stained with Hoechst (blue). Scale bar: 30  $\mu$ m. **E** and **F** Detection of  $\beta$ -III tubulin and GFAP levels by immunoblots (top panels) with their corresponding quantifications (lower panel) normalized with  $\beta$ -actin. **G** Histogram showing the quantification of cell viability using the MTT assay. **A–C** and **E–G**, Black bars represent control (untreated) conditions and grey bars IL-1 $\beta$  treated conditions (10 ng/mL for 24 h). Values for **A–C** are the mean  $\pm$  SEM of 6–8 independent cultures by genotype, for **E** and **F** of 4 independent cultures by genotype and for **G** of 7–3 independent cultures by genotype. Values are presented as % of the control. # $p < 0.05$ , ## $p < 0.01$  and ### $p < 0.001$  between genotypes. ANOVA followed by post hoc Fisher's LSD test. *IB* Immunoblot, *O.D.* optical density



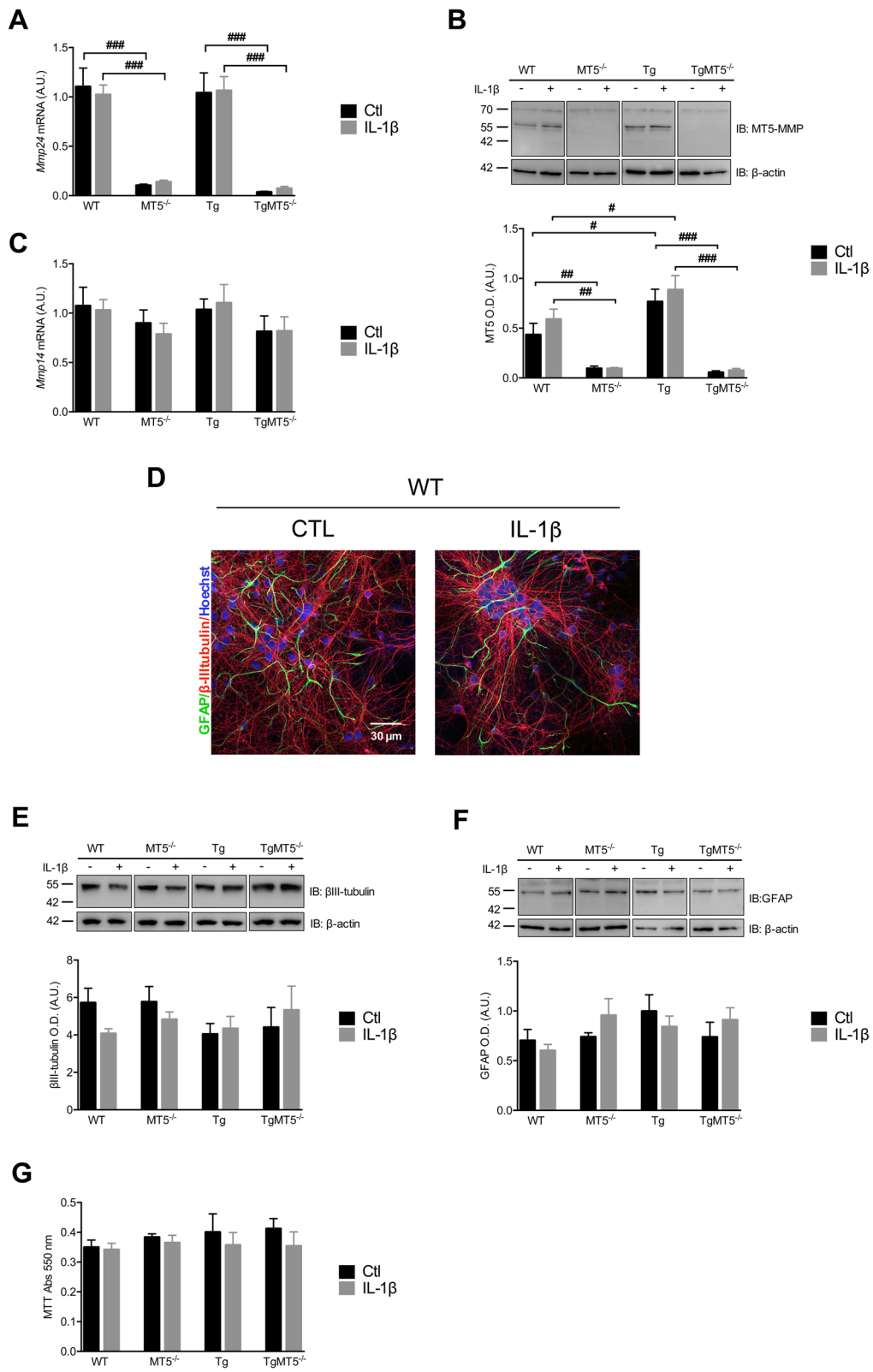


Fig. 1 (See legend on previous page.)



400 by 318% in WT, 79% in MT5<sup>-/-</sup> and 188% in TgMT5<sup>-/-</sup>  
 401 cells, but had no effect in Tg cells, whose *Il-6* levels were  
 402 down by 45% compared to IL-1 $\beta$ -treated WT (Fig. 2G).  
 403 On the contrary, unlike other neuroinflammatory mediators,  
 404 *Tnfa* expression was not affected by IL-1 $\beta$  in the  
 405 present experimental conditions (Fig. 2H). Overall,  
 406 MT5-MMP deficiency modulates the expression of *Il-1 $\beta$* ,  
 407 *Ccl2* and *Il-6* while sparing that of *Tnfa*, which further-  
 408 more is not affected by genotypes or 10 ng/mL of IL-1 $\beta$   
 409 treatment.

#### 410 The levels of MCP-1 and IL-1 $\beta$ proteins decrease 411 in MT5-MMP-deficient cells

412 Considering changes observed at the mRNA level, we  
 413 used ELISA to determine whether protein levels of MCP-  
 414 1, IL-1 $\beta$  and IL-6 were affected by genotype or IL-1 $\beta$   
 415 treatment. Basal MCP-1 levels were below 2000 pg/mL  
 416 in WT and MT5<sup>-/-</sup> cells, while reaching values close to  
 417 3000 pg/mL in Tg cells, which were not significantly dif-  
 418 ferent from WT (Fig. 3A). In contrast, TgMT5<sup>-/-</sup> cells  
 419 exhibited a statistically significant drop (~600 pg/mL)  
 420 of 77% compared with Tg (Fig. 3A). The concentration  
 421 of endogenous IL-1 $\beta$  was around 500 pg/mL in WT and  
 422 MT5<sup>-/-</sup> cells, and 259% higher in Tg cells. Such increase  
 423 was prevented in TgMT5<sup>-/-</sup> cells, whose values were  
 424 87% lower than Tg (Fig. 3B). IL-6 levels were compara-  
 425 tively very low and unchanged in all experimental con-  
 426 ditions (Fig. 3C).

427 Inflammatory challenge with IL-1 $\beta$  strongly upregu-  
 428 lated MCP-1 levels in all genotypes, but they remained  
 429 significantly lower by 29% in TgMT5<sup>-/-</sup> cultures com-  
 430 pared with Tg (Fig. 3D). The burst in IL-1 $\beta$  concen-  
 431 tration detected by ELISA in cell supernatants after  
 432 treatment likely reflects the addition of recombinant  
 433 cytokine, although it cannot be excluded that a small  
 434 portion results from endogenous synthesis. In any case,  
 435 IL-1 $\beta$  levels in TgMT5<sup>-/-</sup> cells were significantly lower  
 436 (45%) compared with Tg (Fig. 3E). IL-6 levels were also  
 437 strongly upregulated by IL-1 $\beta$ , but in this case the major  
 438 change was the 38% reduction in Tg levels compared  
 439 to WT and the recovery of IL-6 levels in TgMT5<sup>-/-</sup>  
 440 cells to near WT values (Fig. 3F). After treatment with  
 441 recombinant IL-1 $\beta$ , a 17 kDa immunoreactive band  
 442 matching the size of the active form of the cytokine,  
 443 and absent in untreated cultures, was detected by WB

444 in cell supernatants, (Fig. 3G). The band intensity was  
 445 reduced in TgMT5<sup>-/-</sup> (62%) and MT5<sup>-/-</sup> (56%) cells,  
 446 compared with Tg and WT, respectively (Fig. 3G). The  
 447 reductions in extracellular IL-1 $\beta$ , prompted us to assess  
 448 its content in cell lysates, inferring a possible increase  
 449 in cellular uptake of the cytokine and consequent intra-  
 450 cellular accumulation. However, this was not the case,  
 451 as cell lysates also revealed a 46% reduction of IL-1 $\beta$   
 452 levels in TgMT5<sup>-/-</sup> cells compared with Tg, while no  
 453 differences were observed between MT5<sup>-/-</sup> and WT  
 454 cells (Fig. 3G).

#### 455 Genotype-dependent degradation of IL-1 $\beta$

456 These results raised the possibility that IL-1 $\beta$  may  
 457 be more efficiently eliminated in the microenviron-  
 458 ment of MT5-MMP-deficient cells. Two MT5-MMP  
 459 homologs, MMP-2 and MMP-9 (also known as gelati-  
 460 nases A and B, respectively), have been shown to  
 461 degrade IL-1 $\beta$ , thus likely contributing to the resolu-  
 462 tion of inflammation under certain circumstances [41].  
 463 We therefore evaluated a compensatory upregulation  
 464 of these soluble MMPs that could explain IL-1 $\beta$  deg-  
 465 radation upon MT5-MMP deficiency. However, no  
 466 changes were observed in the mRNA levels encoding  
 467 MMP-2 and MMP-9 (Fig. 3H). Moreover, a single band  
 468 of gelatinolysis with the expected molecular weight of  
 469 pro-MMP-2 appeared in highly sensitive gelatin zymo-  
 470 grams, and this band remained stable across genotypes  
 471 or after IL-1 $\beta$  treatment (Fig. 3I). The lower molecu-  
 472 lar weight active form of MMP-2 (~64 kDa) and MMP-9  
 473 (~90 kDa) were virtually undetectable in these con-  
 474 ditions (Fig. 3I).

475 We next asked whether, more generally, proteolytic  
 476 activities located in intracellular or extracellular en-  
 477 vironments could explain the putative degradation of  
 478 IL-1 $\beta$ . To this end, we incubated recombinant IL-1 $\beta$  for  
 479 24 h in cell-free conditioned media from cell superna-  
 480 tants or lysates. In this case, IL-1 $\beta$  content remained  
 481 unchanged between genotypes over a 24-h period  
 482 (Fig. 3J). Taken together, these data suggest that recom-  
 483 binant IL-1 $\beta$  is taken up by cells and degraded more  
 484 efficiently intracellularly in MT5-MMP-deficient cells,  
 485 rather than by extracellular proteinases.

(See figure on next page.)

**Fig. 2** Effects of MT5-MMP deficiency on IL-1 $\beta$ -mediated neuroinflammation in cortical neural cell cultures. **A–D** Analyses of *Il-1 $\beta$* , *Ccl2*, *Il-6* and *Tnfa* basal mRNA expression in primary neural cells by RT-qPCR and normalized by *Gapdh* as housekeeping gene. Note the consistent significant decrease of *Il-1 $\beta$* , *Ccl2* and *Il-6* mRNA levels in TgMT5<sup>-/-</sup> cells compared to Tg. **E–H** Analyses of *Il-1 $\beta$* , *Ccl2*, *Il-6* and *Tnfa* mRNA expression in primary neural cells by RT-qPCR and normalized by *Gapdh* as housekeeping gene. Black bars represent control (untreated) conditions and grey bars IL-1 $\beta$  treated conditions (10 ng/mL for 24 h). Values for **A–H** are the mean  $\pm$  SEM of 6–10 independent cultures by genotype. \* $p$  < 0.05, and \*\*\* $p$  < 0.001 between untreated and treated cultures in the same genotype; # $p$  < 0.05 and ## $p$  < 0.01 between genotypes. ANOVA followed by post hoc Fisher's LSD test





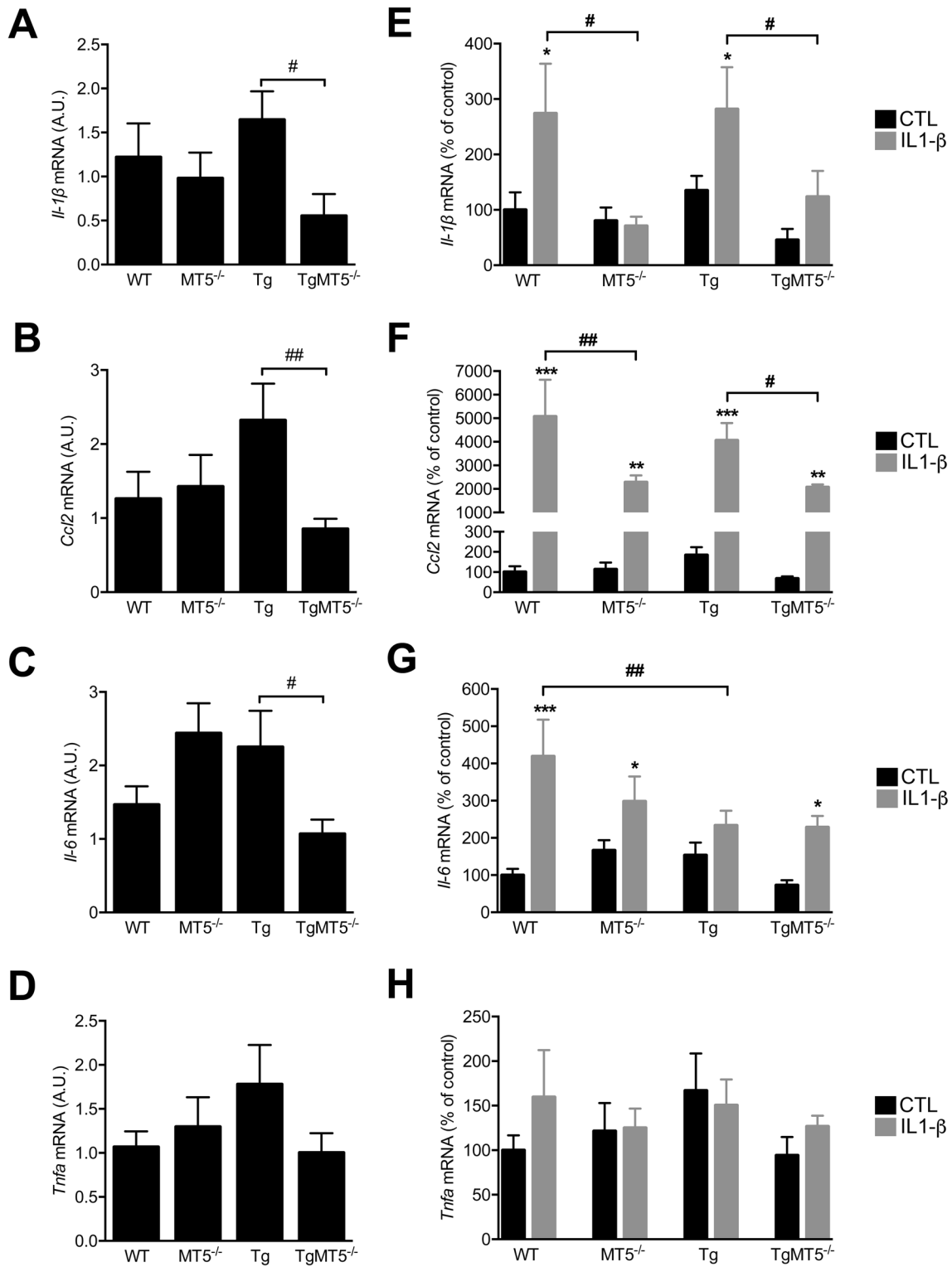


**Fig. 2** (See legend on previous page.)

### Effects of MT5-MMP deficiency and IL-1 $\beta$ on N-cadherin levels and processing

In view of the effects of MT5-MMP deficiency on IL-1 $\beta$  inflammatory response in our cultures, we asked next whether this might be related with a potential deficient processing of MT5-MMP substrate, N-cadherin. The rationale behind this question is that deficient cleavage of N-cadherin in the PNS was reported as a possible mechanism explaining the lack of inflammatory response to IL-1 $\beta$  injection in MT5-MMP-deficient mice [10]. For this reason, we looked for changes in the levels of canonical N-cadherin or its breakdown products resulting from MT5-MMP proteolytic activity. As shown in Fig. 4A, basal levels of full length N-cadherin (NCad FL) remained relatively stable across genotypes (Fig. 4A) and IL-1 $\beta$  treatment did not change this pattern (Fig. 4A and B), suggesting no significant impact of MT5-MMP deficiency on N-cadherin stability. Since N-cadherin breakdown products were not detected, we used a proteasome inhibitor MG132, previously shown to stabilize N-cadherin fragments resulting from MT5-MMP proteolysis [8]. First, we observed that inhibition of the proteasome caused a significant decrease in N-cadherin levels in WT and Tg cells treated with IL-1 $\beta$  and MG132, which could imply the activation of a more efficient degradation pathway, alternative to the proteasome. In MT5<sup>-/-</sup> cells, such decrease was also observed after MG132 treatment alone. Only TgMT5<sup>-/-</sup> cells showed unchanged levels of NCad FL in all experimental conditions (Fig. 4A and B). In agreement with previous report, a C-terminal fragment of ~40 kDa was detected following MG132 treatment [8] (Fig. 4A and C), indicating proteasome degradation of this fragment in normal conditions. The level of N-cadherin 40 kDa (NCad 40 kDa) remained stable across genotypes and treatments except in Tg cells, where combined MG132 and IL-1 $\beta$  caused a 43% decrease compared with MG132 alone. Such decrease was prevented in TgMT5<sup>-/-</sup> cells (Fig. 4A and C), possibly reflecting the relative stability of NCad FL levels in this genotype regardless of the treatment. Taken together, these data suggest that MT5-MMP is unlikely implicated

in N-cadherin processing in our experimental conditions, as its deficiency does not reduce the generation of breakdown products. However, MT5-MMP absence in an inflammatory condition might interfere with the activation of alternative degradation pathways in the case of impaired proteasome function.

### Effects of MT5-MMP deficiency and IL-1 $\beta$ treatment on baseline spontaneous synaptic activity in primary cortical neurons

We and others previously reported that MT5-MMP can modulate neuronal activity [8, 9, 12, 13]. We therefore investigated how the putative functional interaction between MT5-MMP and IL-1 $\beta$  could affect spontaneous synaptic activity of cortical pyramidal cells at 11–14 DIV, when a functional network is already in place [42]. Figure 5A shows a representative snapshot of a recorded pyramidal neuron. In untreated control cultures, membrane capacitance (ranging from 38 to 52 pF) and input resistance (ranging from 590 to 1100 M $\Omega$ ) were monitored after piercing the cell membrane in voltage-clamp mode. Membrane capacitance, which roughly represents the volume of the cell body and proximal branching, was similar across genotypes in untreated conditions. Conversely, IL-1 $\beta$  treatment induced significant increases of membrane capacitance by 72% and 26%, respectively, in MT5<sup>-/-</sup> and in Tg cells compared with their untreated controls (Fig. 5B). In addition, IL-1 $\beta$  increased capacitance in MT5<sup>-/-</sup> and Tg cells by 68% and 32% compared with treated WT cells, respectively. Input resistance is interpreted as a control of the neuron electric integrity, where the differences could highlight qualitative and quantitative changes in ion channels at the membrane surface. In this case, we noted that untreated TgMT5<sup>-/-</sup> cells had a 74% higher input resistance than Tg (Fig. 5C). After IL-1 $\beta$  treatment, no differences were observed between genotypes, which averaged around 500–600 M $\Omega$ , with the notable exception of TgMT5<sup>-/-</sup>, where IL-1 $\beta$  treatment prevented the increase in cell resistance observed in untreated cells (Fig. 5C).

(See figure on next page.)

**Fig. 3** Effects of MT5-MMP deficiency on pro-inflammatory protein levels and IL-1 $\beta$  stability in cortical neural cells. **A–C** Measurement of MCP-1, IL-1 $\beta$  and IL-6 levels (pg/mL) in primary cultures by ELISA. Note the significant decrease of MCP-1 and IL-1 $\beta$  levels in TgMT5<sup>-/-</sup> compared with Tg cells. **D–F** Measurement of MCP-1, IL-1 $\beta$  and IL-6 levels (pg/mL) in primary cultures by ELISA upon IL-1 $\beta$  treatment (10 ng/mL for 24 h). Black bars represent control (untreated) conditions and grey bars IL-1 $\beta$  treated conditions (10 ng/mL for 24 h). **G** Immunoblots (top panel) and the corresponding ponceau normalized quantification (lower panels) of IL-1 $\beta$  levels in supernatants and cell lysates after 24 h of incubation with 10 ng/mL IL-1 $\beta$ . Note that the levels of IL-1 $\beta$  were affected in the absence of MT5-MMP. **H** RT-qPCR analysis of mRNA levels of *Mmp2* (upper panel) and *Mmp9* (bottom panel) in primary cultures normalized by *Gapdh* as housekeeping gene. **I** Zymogram (upper panel) and the corresponding quantification (bottom panel) of pro-MMP-2 levels in primary neural cultures. **J** Immunoblot analyses of IL-1 $\beta$  levels after incubation for 24 h at 37 °C in cell conditioned supernatants and lysates with 10 ng/mL IL-1 $\beta$ . Note that none of the the conditioned media modified IL-1 $\beta$  stability after 24 h incubation. Values for **A–D**, **E** and **H** are the mean  $\pm$  SEM of 6–7 independent cultures by genotype and for **F** and **G** 3–6 independent cultures. Values are presented as % of the control. \* $p$  < 0.05, \*\* $p$  < 0.01 and \*\*\* $p$  < 0.001 between untreated and treated cultures in the same genotype; # $p$  < 0.05, ## $p$  < 0.01 and ### $p$  < 0.001 between genotypes. ANOVA followed by post hoc Fisher's LSD test. *IB* immunoblot, *O.D.* optical density



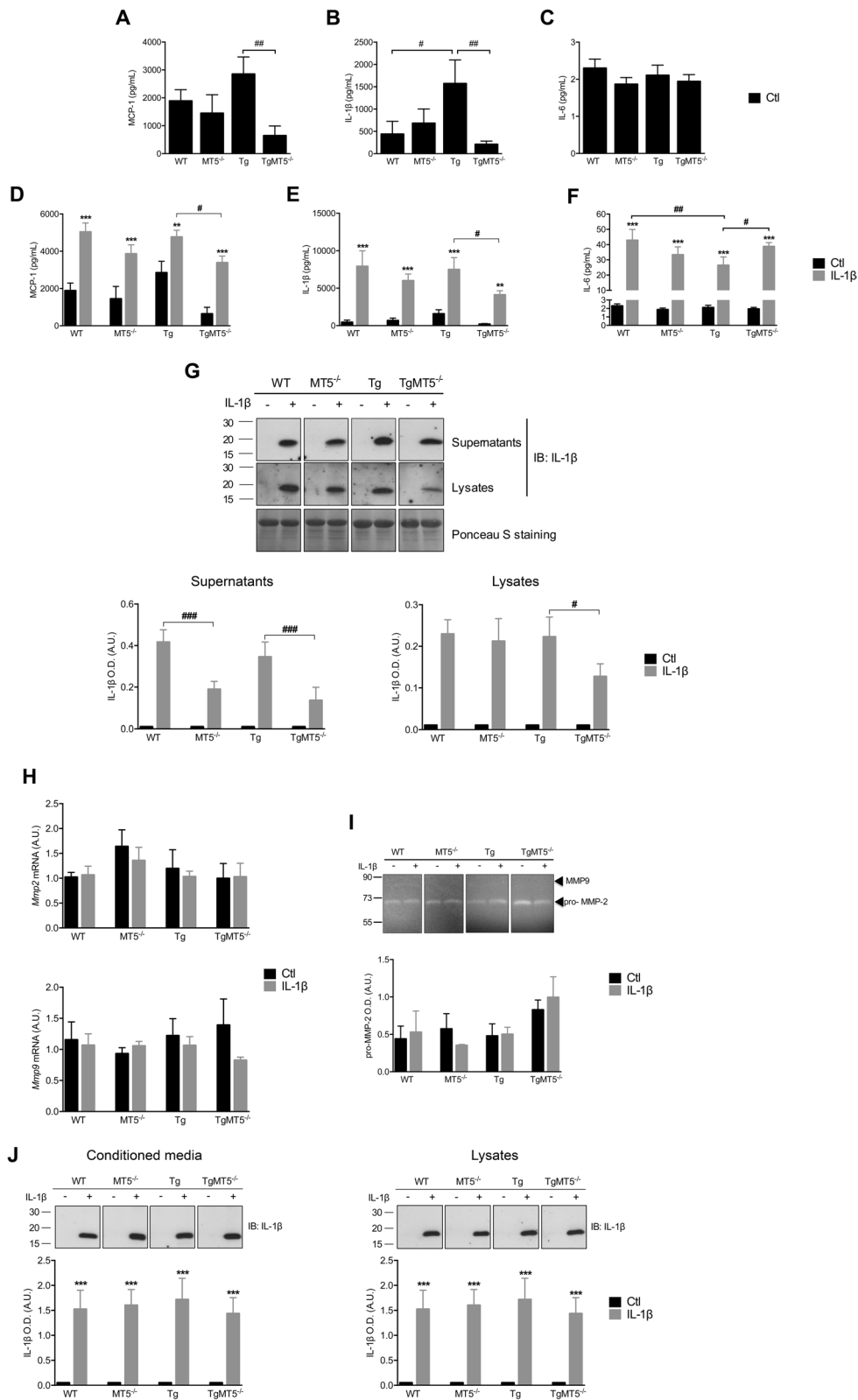
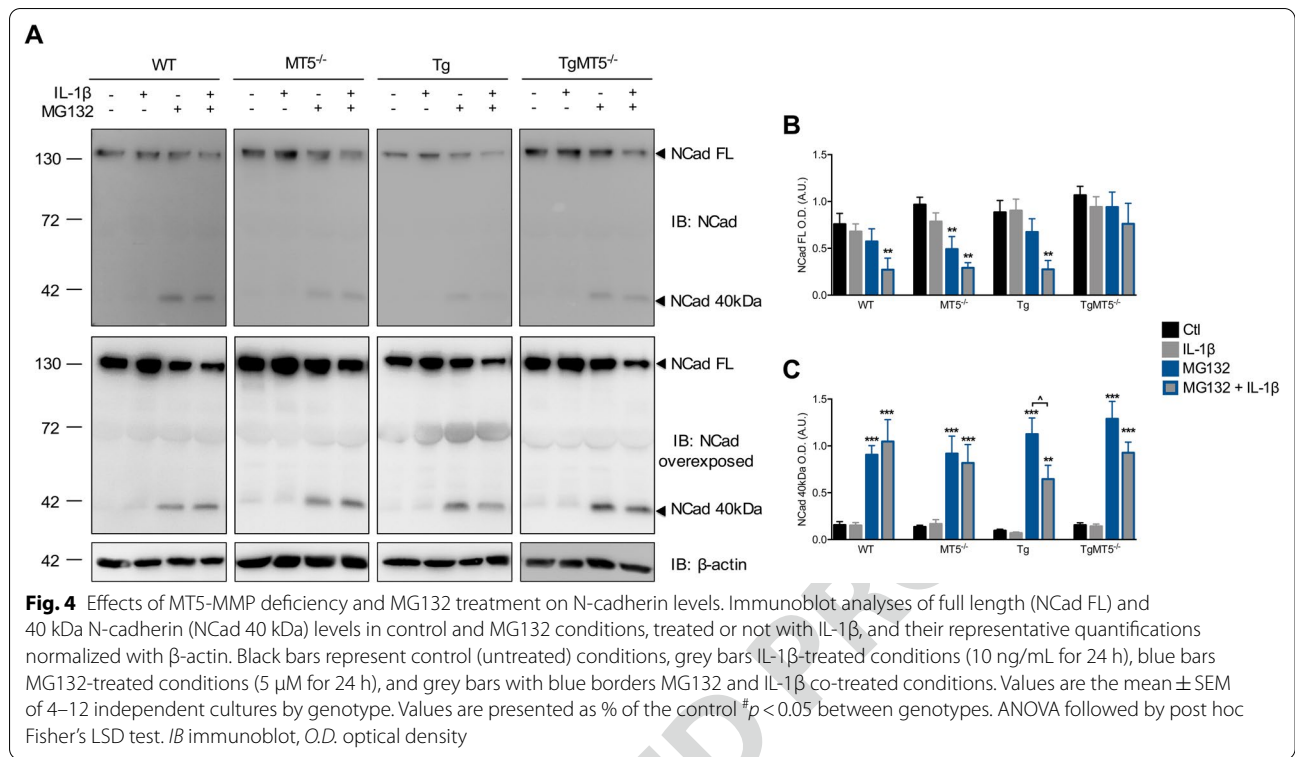


**Fig. 3** (See legend on previous page.)



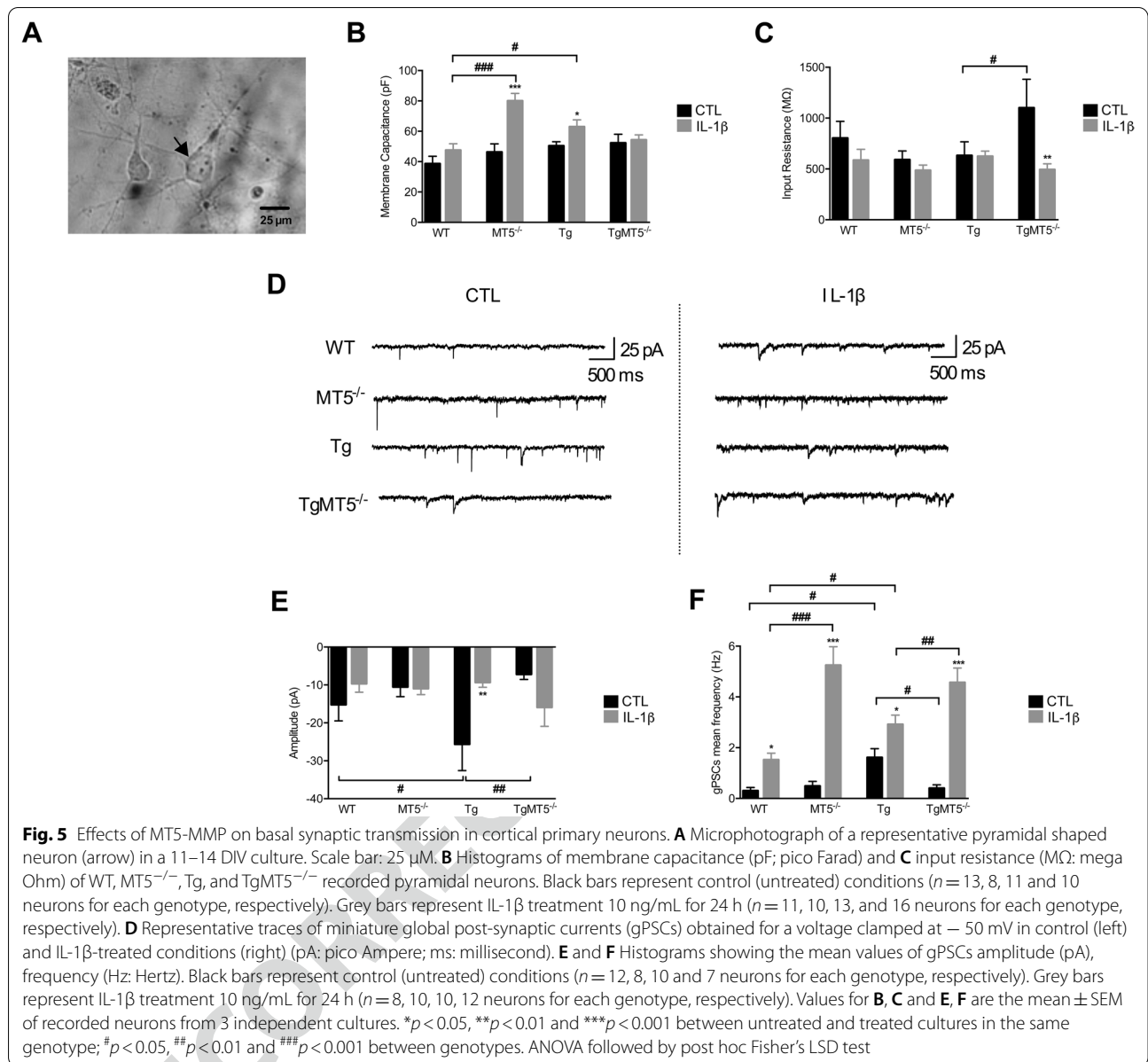


566 Figure 5D shows representative traces for each genotype in untreated (left) and treated (right) cultures. We  
 567 recorded miniature global post-synaptic currents (gPSCs) in gap-free mode during 5 min, with the voltage clamped  
 568 at  $-50$  mV. gPSCs were then analyzed off line and selected individually using the pClamp routine (Fig. 5D).  
 569 The mean peak amplitude of gPSCs ranged from  $-7$  pA to  $-25$  pA, with a maximum value for Tg neurons and  
 570 a minimum for the two MT5-MMP-deficient genotypes (Fig. 5E). The peak amplitude significantly increased by  
 571 69% in untreated Tg neurons compared with WT cells. Such increase was not observed in TgMT5 $^{-/-}$  neurons,  
 572 which had 72% lower levels compared with Tg neurons. Likewise, the increase in peak amplitude in Tg neurons  
 573 was prevented by IL-1 $\beta$ , which decreased levels to 64% of the value in untreated Tg neurons (Fig. 5E). In terms  
 574 of basal event frequency, Tg neurons had a 536% higher value than WT neurons (Fig. 5F). Again, the increase  
 575 was prevented in TgMT5 $^{-/-}$  neurons, where the levels decreased by 75% with respect to Tg. IL-1 $\beta$  treatment  
 576 significantly exacerbated frequency in all genotypes, but the increase was surprisingly particularly important in  
 577 the MT5 $^{-/-}$  and TgMT5 $^{-/-}$  groups, with >1000% in both compared with their untreated controls (Fig. 5F). In comparison,  
 578 frequency augmented by 500% in WT-treated neurons and by only 81% in Tg-treated neurons, relative to their untreated controls (Fig. 5F). Although basal  
 579  
 580  
 581  
 582  
 583  
 584  
 585  
 586  
 587  
 588  
 589  
 590  
 591  
 592

593 frequency was already much higher in Tg cells compared to WT cells, IL-1 $\beta$  was still able to increase frequency in  
 594 Tg cells by nearly twofold (Fig. 5F).  
 595

#### 596 Effects of MT5-MMP deficiency and IL-1 $\beta$ on APP metabolism

597 Changes in inflammatory markers in AD are often associated with the accumulation of A $\beta$  following amyloidogenic  
 598 processing of APP [43, 44]. Knowing that MT5-MMP can modulate APP/A $\beta$  metabolism [13, 17], we asked whether the  
 599 apparent pro-inflammatory action of MT5-MMP might result from its ability to stimulate APP metabolism and A $\beta$  accumulation.  
 600 To address this question, we first measured the levels of secreted (sAPP) or cellular full-length APP (APPfl) using an antibody  
 601 directed against the N-terminal portion of APP (i.e., 22C11). This revealed no change in sAPP levels between  
 602 genotypes, and only a significant decrease of 27% for APPfl in TgMT5 $^{-/-}$  cells compared with Tg (Fig. 6A).  
 603 Treatments with IL-1 $\beta$  and/or  $\gamma$ -secretase inhibitor DAPT did not affect sAPP or APPfl levels (Fig. 6A).  
 604 DAPT was primarily intended to block  $\gamma$ -secretase-mediated processing of CTFs to stabilize them and thus  
 605 facilitate their detection. This was important to compare our experimental setting with in vivo work reporting  
 606 brain accumulation of C99 preceding that of A $\beta$  in 3xTg and 5xFAD mouse models of AD [34, 45], as well as the  
 607  
 608  
 609  
 610  
 611  
 612  
 613  
 614  
 615  
 616  
 617  
 618



(See figure on next page.)

**Fig. 6** Effects of MT5-MMP deficiency and IL-1 $\beta$  on APP metabolism in cortical neural cell cultures. **A** Immunoblot analyses of soluble APP (sAPP) and canonical full length APP (APP<sub>FL</sub>) detected with the 22C11 antibody in primary cultures untreated and treated or not with IL-1 $\beta$  (10 ng/mL) and/or DAPT (10  $\mu$ M), and the corresponding  $\beta$ -actin normalized quantifications. **B** Immunoblot analyses of APP CTF fragments detected with APP-CTF antibody in primary cultures untreated and treated or not with IL-1 $\beta$  (10 ng/mL) and/or DAPT (10  $\mu$ M), and the corresponding  $\beta$ -actin normalized quantifications. AAV-C99 (right) indicates a positive control. WT cells were infected for 5 days with AAV-C99 and recovered at 11 DIV. Note that only C83 levels were detectable with DAPT treatment. **C** and **D** Measurement by MSD multiplex assay of A $\beta$ 40 and A $\beta$ 42 levels (pg/mL) in primary cultures in control (black) and IL-1 $\beta$  (grey) conditions. Values are the mean  $\pm$  SEM of 8–16 for **A**, **B** and 4–5 for **C**, **D** independent cultures by genotype. \* $p < 0.05$  and \*\*\* $p < 0.001$  between untreated and treated cultures with IL-1 $\beta$  and DAPT in the same genotype; # $p < 0.05$ , ## $p < 0.01$  between genotypes. ANOVA followed by post hoc Fisher's LSD test. *B* immunoblot, *O.D.* optical density, *A.U.* arbitrary units



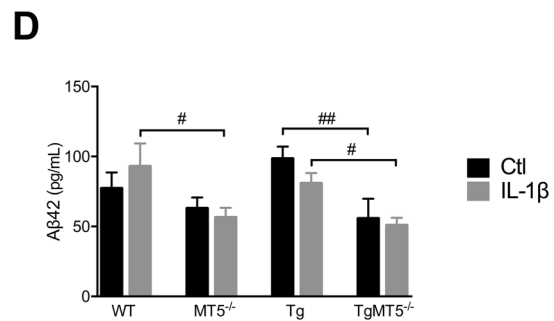
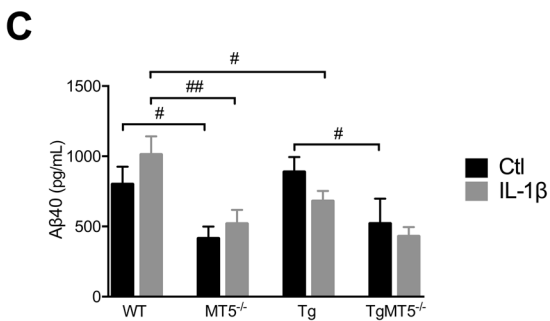
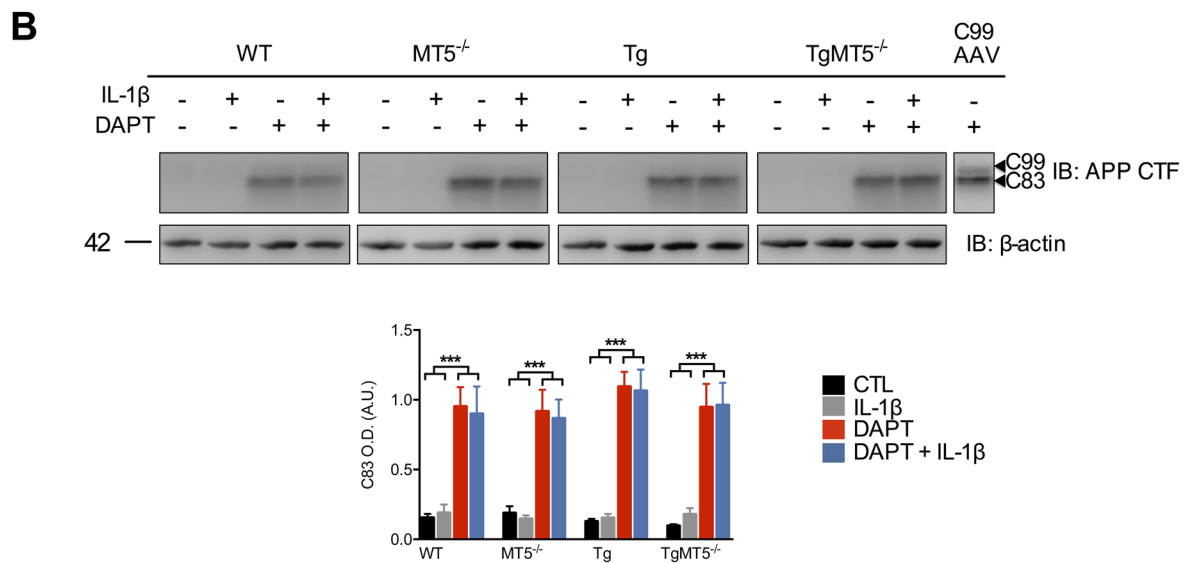
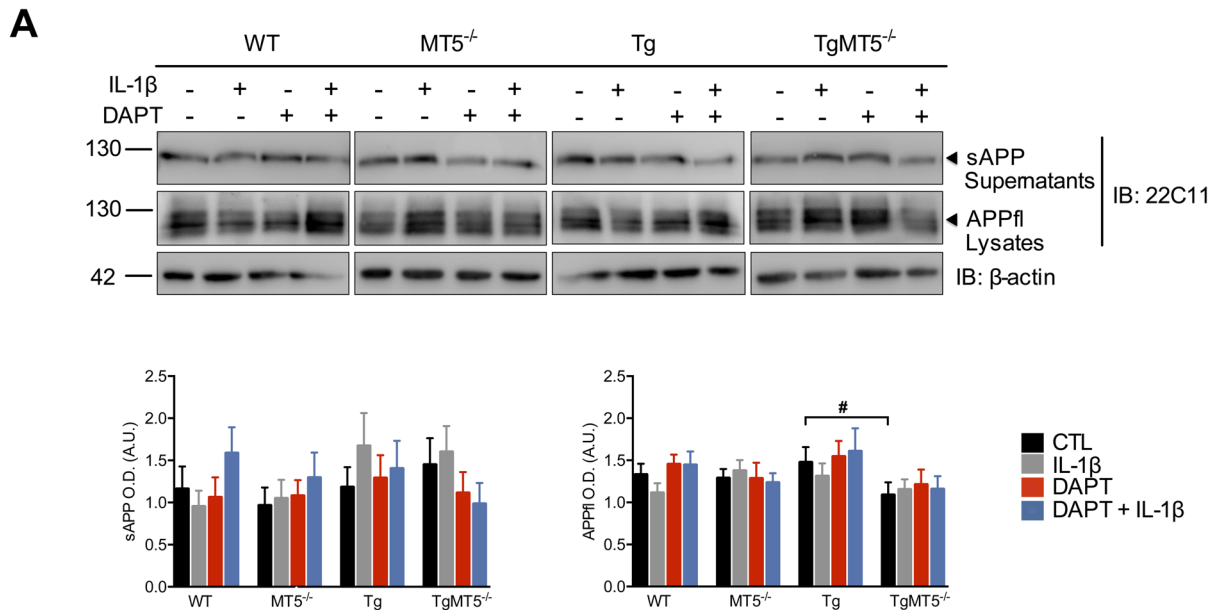


**Fig. 6** (See legend on previous page.)



619 decrease of C99 and C83 upon MT5-MMP deficiency in  
 620 5xFAD mice [13, 17]. After DAPT and immunoblot with  
 621 the APP CTF antibody, we detected a single band corre-  
 622 sponding to the expected size of C83 that was not altered  
 623 by MT5-MMP deficiency or IL-1 $\beta$  treatment (Fig. 6B). In  
 624 contrast, no band corresponding to the size of C99 was  
 625 detected with any of the three antibodies tested: APP-  
 626 CTF (Fig. 6B), 6E10 (which recognizes human APP and  
 627 its fragments containing the N-terminal of C99; data not  
 628 shown) or 82E1, which recognizes the neopeptide in the  
 629 N-terminal of C99/A $\beta$  (Asp1) generated by  $\beta$ -secretase  
 630 cleavage (data not shown). The absence of C99 was fur-  
 631 ther confirmed after subcellular fractioning of membra-  
 632 nous, cytosolic and nuclear compartments (Additional  
 633 file 2). In contrast, C83 was slightly detected only at the  
 634 membrane in control conditions but its levels dramati-  
 635 cally increased upon DAPT treatment in this fraction,  
 636 and interestingly, also in the nucleus, although to a lesser  
 637 extent (Additional file 2). It is noteworthy that the APP-  
 638 CTF and 6E10 antibodies did not detect any immuno-  
 639 reactive band around 30–40 kDa compatible with the  
 640 expected size of the  $\eta$ -CTF fragments.

641 Next, we measured the levels of murine A $\beta$ 38, A $\beta$ 40  
 642 and A $\beta$ 42. A $\beta$ 38 was not detected in our cultures (not  
 643 shown) and we found no increase of either species in Tg  
 644 compared with WT cultures (Fig. 6C). However, MT5-  
 645 MMP deficiency significantly reduced A $\beta$ 40 levels in  
 646 MT5 $^{-/-}$  (48%) and TgMT5 $^{-/-}$  (41%) cells, compared  
 647 with WT and Tg cells, respectively (Fig. 6C). Although  
 648 IL-1 $\beta$  did not affect intragenotype A $\beta$ 40 levels, it caused  
 649 a significant reduction in Tg (33%) and MT5 $^{-/-}$  cells  
 650 (49%) compared with WT (Fig. 6C). Basal A $\beta$ 42 levels  
 651 were approximately tenfold lower than those of A $\beta$ 40.  
 652 The lack of MT5-MMP in this case reduced by 44% the  
 653 levels of A $\beta$ 42 only in TgMT5 $^{-/-}$  cells compared with Tg  
 654 (Fig. 6D). IL-1 $\beta$  had not effect on A $\beta$  levels (Fig. 6C and  
 655 D). We conclude that MT5-MMP deficiency downregu-  
 656 lates A $\beta$ 40 and A $\beta$ 42 levels in developing neural cells in  
 657 culture and that this trend is not modified by IL-1 $\beta$  after  
 658 24 h of incubation.

659 Human A $\beta$ 40 was detected only in Tg and TgMT5 $^{-/-}$   
 660 cells, albeit at relatively low concentrations ( $\sim$ 35 pg/mL),  
 661 as revealed by a human-specific ELISA kit (Additional  
 662 file 1A), indicating that the Thy1 neuronal promoter was  
 663 functional to drive human transgene expression and effi-  
 664 cient metabolism of human APP. This is consistent  
 665 with previous data showing activation of the Thy1 pro-  
 666 moter at 4–5 DIV [46] and with the detection of *hAPP*  
 667 and *hPSEN1* mRNAs in our cultures (Additional file 1B  
 668 and C). Genotype or IL-1 $\beta$  treatment did not affect the  
 669 content of hA $\beta$ 40, *hAPP* or *hPSEN1* gene expression  
 670 in any way in our experimental conditions (Additional  
 671 file 1A–C).

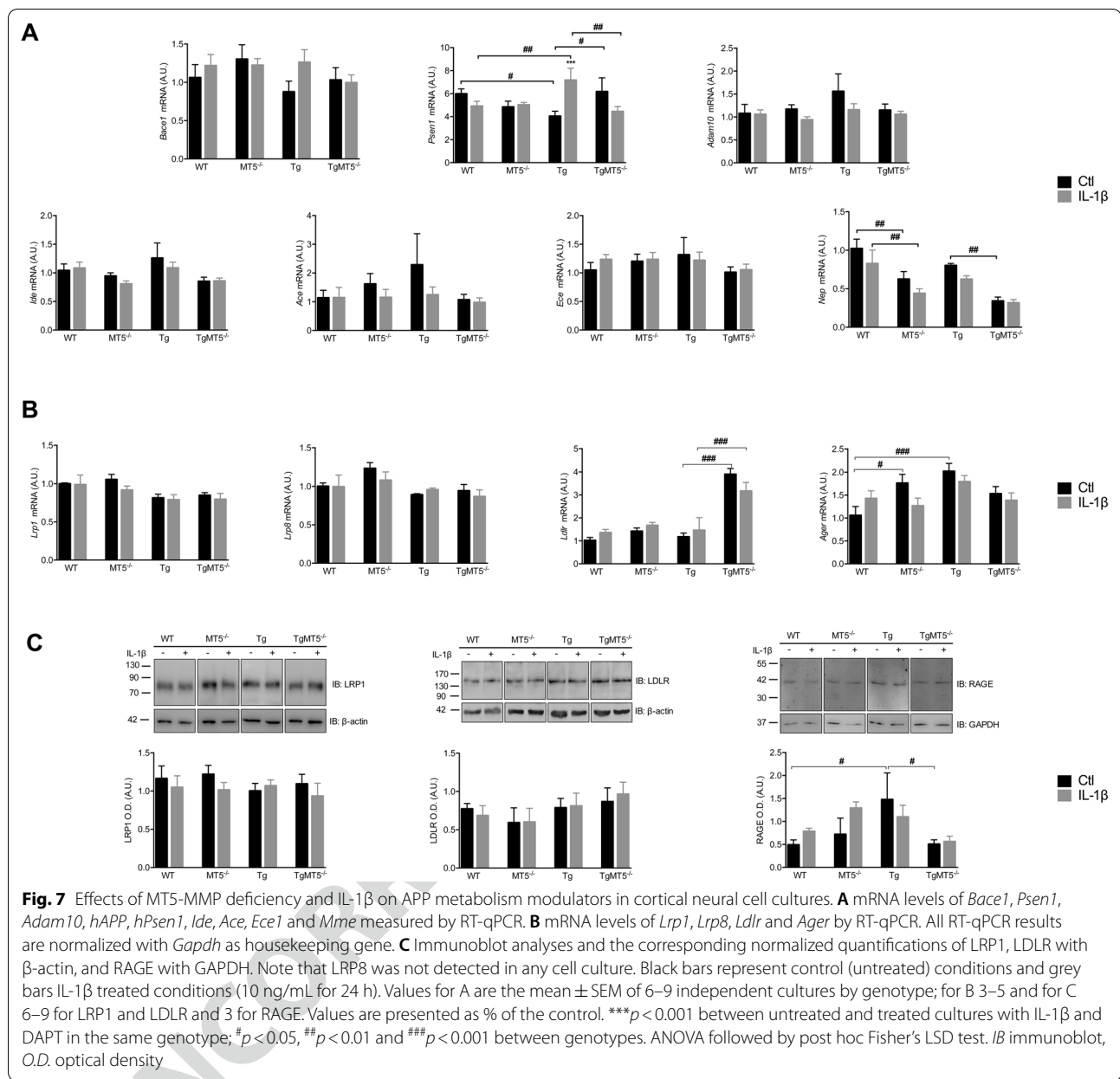
## 672 Expression of genes involved in A $\beta$ production 673 and degradation

674 Because A $\beta$  content results from a balance between pro-  
 675 duction and degradation, we assessed possible changes  
 676 in the gene expression of enzymes implicated in these  
 677 processes, e.g., BACE1 (*Bace1*), presenilin 1 (*Psen1*),  
 678 ADAM10 (*Adam10*), insulin-degrading enzyme (*Ide*),  
 679 angiotensin-converting enzyme (*Ace*), endothelin-con-  
 680 verting enzyme (*Ece*) and neprilysin (*Mme*). Only *Psen1*  
 681 and *Mme* showed significant changes. In basal condi-  
 682 tions, Tg cells expressed 33% lower levels of *Psen1*  
 683 mRNA compared with WT cells and 35% lower compared  
 684 with TgMT5 $^{-/-}$  cells. IL-1 $\beta$  induced a 79% increase of  
 685 *Psen1* mRNA levels in Tg compared with untreated cells,  
 686 and this increase was also significant when compared to  
 687 WT (46%) and TgMT5 $^{-/-}$  cells (60%) under the same  
 688 conditions (Fig. 7A). *Mme* expression was clearly down-  
 689 regulated in the absence of MT5-MMP. In MT5 $^{-/-}$  and  
 690 TgMT5 $^{-/-}$  cells, *Mme* mRNA was down by 40% and 58%  
 691 compared with untreated WT and Tg cells, respectively.  
 692 IL-1 $\beta$  did not significantly modify the intragenotype  
 693 values, but significant decreases of 47% and 49% were  
 694 observed in MT5 $^{-/-}$  and TgMT5 $^{-/-}$  cells, compared with  
 695 WT and Tg cells, respectively (Fig. 7A).

696 Cellular receptors such as low-density lipoprotein  
 697 receptor-related protein 1 (LRP1) [47–50], LRP8 [51],  
 698 LDLR [52] or RAGE [53] may also affect APP metabolism  
 699 by either modulating the activities of  $\beta$ - and  $\gamma$ -secretase  
 700 and/or directly A $\beta$  levels through endocytosis. In this  
 701 context, *Lrp1* and *Lrp8* mRNA expression was stable  
 702 in all experimental groups (Fig. 7B). In contrast, *Ldlr*  
 703 mRNA content was significantly upregulated by 231%  
 704 in TgMT5 $^{-/-}$  compared with Tg, and IL-1 $\beta$  did not alter  
 705 this trend. The RAGE receptor encoded by the *Ager* gene,  
 706 showed no differences upon IL-1 $\beta$  stimulation. Never-  
 707 theless, under basal conditions, MT5 $^{-/-}$  and Tg cells  
 708 expressed significantly more *Ager* than WT cells (67%  
 709 and 92%, respectively) (Fig. 7B). Next, we assessed the  
 710 protein content of these receptors by WB. In our experi-  
 711 mental conditions, LRP8 was undetectable and no differ-  
 712 ences were observed between genotypes and treatment  
 713 for LRP-1 and LDLR (Fig. 7C). Tg cultures expressed sig-  
 714 nificantly higher levels of RAGE compared to WT (200%)  
 715 and TgMT5 $^{-/-}$  (194%) (Fig. 7C). IL-1 $\beta$  treatment did not  
 716 modulate RAGE content in all genotypes.

717 Overall, there was no clear evidence of transcriptional  
 718 regulations that could explain the downregulation of A $\beta$   
 719 content upon MT5-MMP deficiency. The results also  
 720 indicated that incubation of 10 ng/mL of IL-1 $\beta$  for 24 h  
 721 did not impact the expression of genes encoding poten-  
 722 tial modulators of A $\beta$  balance, and confirmed overall no  
 723 influence of the cytokine in global APP/A $\beta$  metabolism  
 724 in our experimental settings.



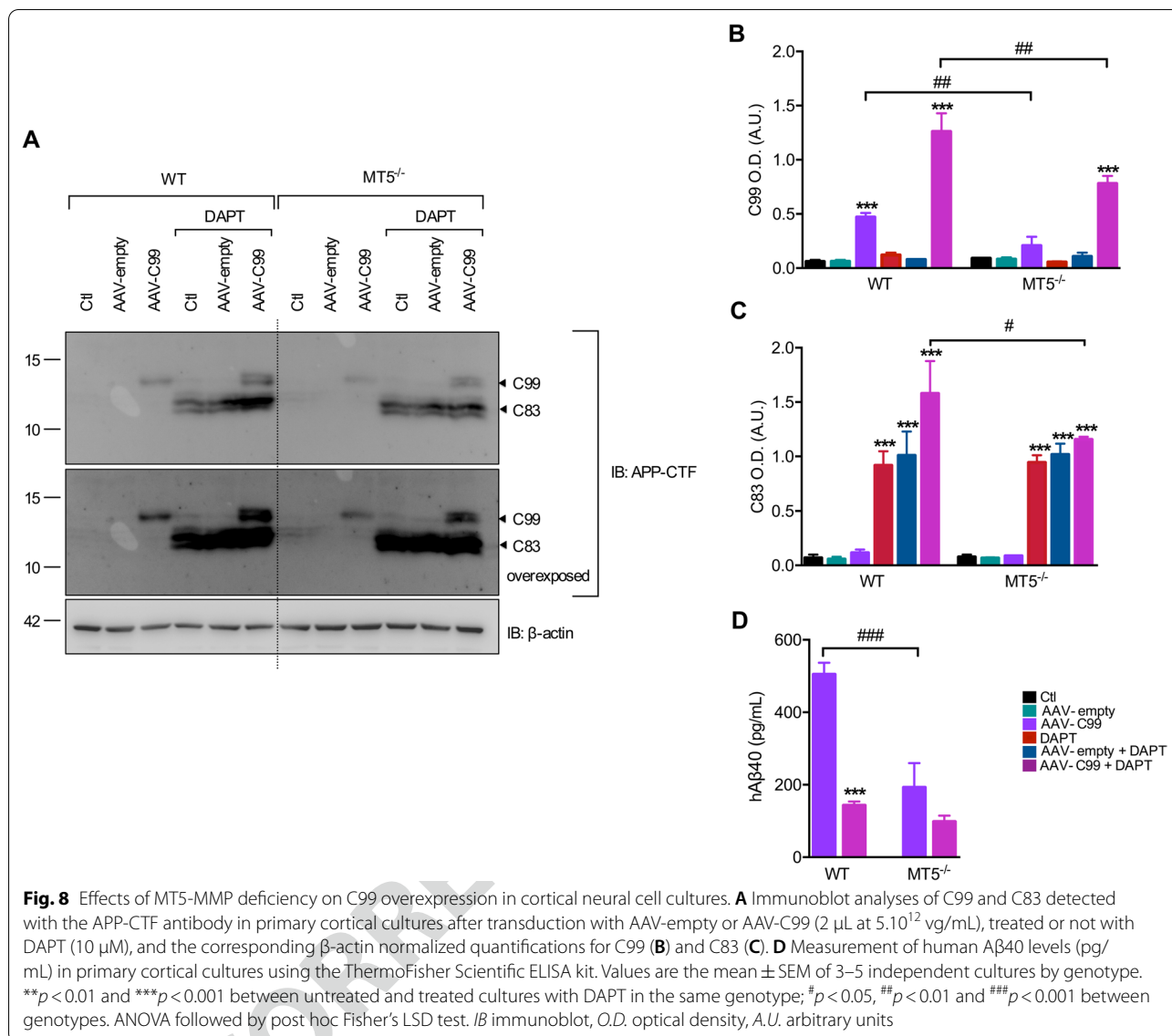


725 **Overexpression of C99 reveals the potential of MT5-MMP**  
 726 **to control its accumulation in CNS cells**

727 Under our experimental conditions, the incipient expres-  
 728 sion of *hAPP* and *hPSEN1* transgenes carrying AD muta-  
 729 tions and/or acute IL-1 $\beta$  challenge were not sufficient  
 730 to trigger the accumulation of C99 characteristic of AD,  
 731 although MT5-MMP deficiency downregulated A $\beta$  levels.  
 732 These data likely reflect extreme lability and/or rela-  
 733 tively low production of endogenous C99 in developing  
 734 neurons. Taken together, this could contribute to the  
 735 inability to detect steady-state C99 levels and thus mask  
 736 a putative impact of MT5-MMP in C99 metabolism, as

737 previously shown in adult 5xFAD mice [13, 17]. To cir-  
 738 cumvent this difficulty and assess whether MT5-MMP  
 739 could actually regulate C99 levels in developing neurons,  
 740 we overexpressed human C99 in WT and MT5<sup>-/-</sup> cul-  
 741 tures using an AAV-C99 under the control of the neuron-  
 742 specific synapsin promoter [29]. As shown in Fig. 8A–C,  
 743 in non-transduced cells or in cells transduced with an  
 744 empty AAV, CTFs did not spontaneously accumulate and  
 745 DAPT rescued only C83, but not C99 levels, consistent  
 746 with C83 being a preferential substrate of  $\gamma$ -secretase [32]  
 747 and the most abundant APP fragment in cultured neu-  
 748 rons [15, 16]. Furthermore, MT5-MMP deficiency did





749 not alter basal C83 after DAPT treatment (Fig. 8A and  
 750 C), mirroring results in Fig. 6B. As expected, neurons  
 751 transduced with AAV-C99 accumulated C99 and, most  
 752 interestingly, its levels were significantly reduced by 56%  
 753 in MT5<sup>-/-</sup> cells compared with WT cells (Fig. 8A and B).  
 754 C83 was undetectable in DAPT-free conditions (Fig. 8A  
 755 and C). Conversely, DAPT treatment caused a 168% and  
 756 1300% increase in C99 and C83 in WT cells compared to  
 757 untreated AAV-C99 cells, respectively (Fig. 8A–C). This  
 758 high accumulation of CTFs was significantly reduced  
 759 in MT5<sup>-/-</sup> cells by 39% for C99 and 38% for C83. Consistent  
 760 with these data, ELISA showed a 62% decrease of human  
 761 A $\beta$ 40 levels in MT5<sup>-/-</sup> cells transduced with AAV-C99,  
 762 compared with WT (Fig. 8D). As anticipated, DAPT nearly  
 763 blocked A $\beta$  formation from C99 in

749 WT cells (Fig. 8D), whereas the effect was negligible on  
 750 MT5<sup>-/-</sup> cells because their A $\beta$  content was already very  
 751 low (Fig. 8D). We conclude that MT5-MMP deficiency  
 752 effectively prevents the accumulation of a major patho-  
 753 genic feature of AD and, more interestingly, that this can  
 754 occur in developing neural cells.  
 755

### 770 Discussion

771 This study provides the first experimental evidence that  
 772 MT5-MMP deficiency tunes down neuroinflammation,  
 773 APP metabolism and neuronal excitability in primary  
 774 cortical cultures of AD and non-AD mice. This occurs  
 775 as early as 11 DIV, with stable neuronal and astrocyte  
 776 markers across genotypes, and upregulated levels of  
 777 MT5-MMP in Tg cells. We found no clear evidence of

778 cross-regulation between neuroinflammation and APP  
 779 metabolism in young neural cells, as the effects of MT5-  
 780 MMP deficiency on downregulation of IL-1 $\beta$  signaling  
 781 and A $\beta$  production were not cumulative. In addition,  
 782 neuroinflammation caused by IL-1 $\beta$  treatment did not  
 783 impact the levels of APP metabolites (e.g., A $\beta$  and APP  
 784 CTFs), which were instead controlled by the presence or  
 785 absence of MT5-MMP. Proteinase deletion also prevents  
 786 spontaneous hyperexcitability in Tg neurons, but para-  
 787 doxically exacerbates the frequency of events upon IL-1 $\beta$   
 788 treatment. Overall, MT5-MMP appears to be an enzyme  
 789 capable of controlling different physiological and patho-  
 790 logical pathways, the latter set in motion by the nascent  
 791 expression of human AD transgenes in developing neural  
 792 cells 11 days seeding. This confirms the beneficial effect  
 793 of MT5-MMP modulation on the early cellular dysfunc-  
 794 tions identified, which are likely precursors to the patho-  
 795 genesis of AD.

#### 796 **MT5-MMP is upregulated in Tg cultures and its deficiency** 797 **does not affect cell culture composition**

798 An important finding of this work is that MT5-MMP  
 799 content is higher in Tg cells, suggesting a modulating  
 800 effect of AD transgenes on proteinase. Such regulation  
 801 highlights that the impact of MT5-MMP in AD, previ-  
 802 ously described in adult mice [13, 17], may actually begin  
 803 at a stage well before the onset of obvious pathological  
 804 and clinical signs. Of note, MT5-MMP deletion did not  
 805 alter the expression of MT1-MMP, MMP-9 or MMP-2,  
 806 all close MT5-MMP homologues, also involved in the  
 807 control of APP metabolism and amyloidogenesis [33, 34,  
 808 54, 55], implying no compensatory regulation by these  
 809 proteinases upon MT5-MMP deficiency. The content of  
 810  $\beta$ -III tubulin and GFAP, as well as the values of the  
 811 MTT test, were similar across all experimental groups.  
 812 This lack of cytotoxicity contrasts with a previous report  
 813 showing cell demise in 5xFAD primary cortical neurons  
 814 at 7 DIV [56]. In this study, no astrocytes were reported  
 815 and cell density was fivefold lower than ours, which could  
 816 explain a microenvironment that facilitates neuronal vul-  
 817 nerability. In addition, the apparent lack of toxicity medi-  
 818 ated by IL-1 $\beta$  compared to previous studies [57, 58] may  
 819 be related to different experimental settings used, includ-  
 820 ing concentrations and time of exposure to the cytokine.

#### 821 **MT5-MMP deficiency attenuates basal neuroinflammation** 822 **and the neuroinflammatory response to IL-1 $\beta$ in CNS** 823 **neural cells**

824 We previously found increased levels of IL-1 $\beta$  in the  
 825 brain of 3-day 5xFAD old pups [59] prior A $\beta$  accumula-  
 826 tion, and later at 2 months, along with the onset of A $\beta$   
 827 accumulation [34]. Interestingly, MT5-MMP deletion  
 828 resulted in decreased IL-1 $\beta$  levels in the brains of 5xFAD

829 mice at prodromal stages of the pathology, indicating  
 830 functional interactions between IL-1 $\beta$  and MT5-MMP  
 831 [13]. Consistent with this idea, we show here that basal  
 832 IL-1 $\beta$  levels are higher in Tg cells and stable A $\beta$  content  
 833 compared to WT, arguing for regulation of inflammation  
 834 in young cells by a non-A $\beta$  related mechanism. Moreover,  
 835 MT5-MMP deficiency reduces the neuroinflammatory  
 836 response to IL-1 $\beta$  as well as the basal levels of IL-1 $\beta$  and  
 837 MCP-1. The effect of genotype/IL-1 $\beta$  was cytokine-selec-  
 838 tive, as shown by the lack of effect on *Tnfa*, and a more  
 839 complex behavior of IL-6, whose reduction in Tg cells  
 840 after IL-1 $\beta$  was recovered in TgMT5<sup>-/-</sup>. Downregulation  
 841 of MCP-1 in MT5-MMP-deficient cells could dampen  
 842 the system's ability to recruit microglia/macrophages  
 843 to the site of inflammation, thereby helping to limit the  
 844 progression of an exacerbated inflammatory response.  
 845 Overall, these data echo a previous study showing that  
 846 systemic injection of IL-1 $\beta$  did not trigger an inflamma-  
 847 tory response in the PNS of adult MT5-MMP-deficient  
 848 mice [10]. In that case, MT5-MMP-deficient prevented  
 849 proper N-cadherin processing eventually disrupting the  
 850 crosstalk between sensory neurons and mast cells [10].  
 851 Unchanged levels of N-cadherin or its proteolytic frag-  
 852 ments in our MT5-MMP-deficient cells argue against  
 853 this possibility. Alternatively, our data imply *instead* that  
 854 cells lacking MT5-MMP could degrade IL-1 $\beta$  in a more  
 855 efficient manner. This idea is indirectly supported by  
 856 recent data showing that non-catalytic interactions of  
 857 MT5-MMP promote C99 degradation by the proteasome  
 858 and, to a lesser extent, by lysosomes [32]. Although IL-1 $\beta$   
 859 clearance is not well understood, it has been suggested  
 860 that low levels of IL-1 $\beta$  stimulate autophagolysosomal  
 861 function and attenuate inflammation in cell cultures,  
 862 while higher cytokine concentrations (> 200 pg/mL) have  
 863 the opposite effect [60, 61]. Whether MT5-MMP may  
 864 act as an interactor/chaperon for IL-1 $\beta$  and/or the IL-1 $\beta$ /  
 865 IL-1R1 complex, as it is the case for APP [13, 17, 32],  
 866 needs further investigation.

#### 867 **Changes in spontaneous synaptic activity depend** 868 **on genotype and IL-1 $\beta$ treatment**

869 To investigate the impact of MT5-MMP deficiency on  
 870 basal synaptic activity, we measured spontaneous net-  
 871 work synaptic events as a landmark for each genotype.  
 872 In agreement with previous reports (see for review  
 873 [62]), our Tg (5xFAD) neurons showed increased syn-  
 874 aptic activity, as illustrated by higher amplitude and  
 875 frequency, which is considered as a sign of hyperex-  
 876 citability. At 11–14 DIV, with WT and Tg cells show-  
 877 ing equal levels of A $\beta$  (see Fig. 6), it is unlikely that  
 878 the peptide influences the hyperexcitability observed  
 879 in Tg neurons. The latter showed increased levels of  
 880 MT5-MMP and IL-1 $\beta$  compared with WT, and more



881 interestingly TgMT5<sup>-/-</sup> neurons do not show hyper-  
 882 excitability and show control values of IL-1 $\beta$  levels.  
 883 Together, this raises the possibility of a coordinated  
 884 action of MT5-MMP and IL-1 $\beta$  in promoting neu-  
 885 ronal hyperexcitability. Although, IL-1 $\beta$  has diverse  
 886 and sometimes divergent effects on neuronal activity  
 887 depending on cell-type, cytokine concentration and  
 888 duration of the stimulus [63], several studies highlight  
 889 various mechanisms of IL-1 $\beta$ -mediated excitability:  
 890 NMDA receptor stimulation of Ca<sup>2+</sup> influx [64], inhi-  
 891 bition of GABA-evoked currents [65] or prevention of  
 892 the inhibitory effect of cannabinoid CB1 receptor on  
 893 glutamate release [66]. In this context, it is possible  
 894 that the onset of neuronal hyperexcitability observed  
 895 in 5xFAD mice [67, 68] takes place during develop-  
 896 ment, in which case, lower levels of IL-1 $\beta$  in MT5-  
 897 MMP-deficient neurons could help to attenuate this  
 898 process in the long run.

899 IL-1 $\beta$  elicited cell responses such as prevent-  
 900 ing an increase in amplitude in Tg cells, which could  
 901 be interpreted as a homeostatic cellular response  
 902 to the inflammatory burst. A possible post-synaptic  
 903 mechanism of IL-1 $\beta$  underlying such effect could be  
 904 the cytokine-mediated decrease in the content and  
 905 phosphorylation of the AMPA-GluR1 subunit at the  
 906 post-synaptic membrane [69]. IL-1 $\beta$  may also act as  
 907 pre-synaptic neuromodulator [70, 71], which is con-  
 908 sistent with the increased frequency we observed in  
 909 all genotypes. However, the magnitude of the effect  
 910 of MT5-MMP deficiency is surprising, given the weak  
 911 inflammatory response of MT5<sup>-/-</sup> cells to IL-1 $\beta$  (see  
 912 Fig. 3), raising the possibility that MT5-MMP could  
 913 differentially affect various IL-1 $\beta$  signaling pathways  
 914 mediated [63] or not [72] by membrane receptors.  
 915 Furthermore, as the increase in capacitance corre-  
 916 lates with the increase in membrane surface area and  
 917 pre-synaptic vesicle fusion [69], a parallelism could be  
 918 established with the observation of increased gPSCs  
 919 and capacitance in IL-1 $\beta$ -treated MT5<sup>-/-</sup> neurons.  
 920 However, no general conclusion can be drawn, as this  
 921 correlation was not validated in the other experimen-  
 922 tal groups. Alternatively, the lack of MT5-MMP could  
 923 prevent the formation of sAPP95/sAPP $\eta$ , recently sug-  
 924 gested to bind the GABA<sub>B</sub>R1a and inhibit pre-syn-  
 925 aptic neurotransmitter release [73]. Even if we found  
 926 no sAPP around 85–95 kDa, we cannot exclude that  
 927 a small functional pool of this WB-undetectable frag-  
 928 ment reaches the synapse. Although further research is  
 929 needed to better understand the novel effects reported  
 930 here, MT5-MMP deficiency appears to prevent AD  
 931 genotype-related synaptic dysfunction under basal  
 932 conditions, while exacerbating IL-1 $\beta$ -induced neu-  
 933 ronal excitability.

### 934 MT5-MMP deficiency reduces A $\beta$ levels and has no effect 935 on endogenous CTFs

936 In contrast to previous observations in the brains of  
 937 adult 5xFAD mice [13, 17, 34], C99 did not accumulate  
 938 in developing neural cells. Yet, murine A $\beta$  implicitly  
 939 proved the formation at some point of its immediate  
 940 precursor, C99. We assume that the latter is formed  
 941 a low pace and/or that it is promptly degraded by the  
 942 proteasome or autophagolysosome [32], and even by  
 943  $\alpha$ -secretase to yield C83 [32, 74]. Likely, all or some of  
 944 these mechanisms are active in developing neural cells,  
 945 thus preventing the neurotoxic effects of C99 accumu-  
 946 lation [29, 45, 75]. In contrast to C99, DAPT did res-  
 947 cue C83 levels, which were not altered by MT5-MMP  
 948 deficiency. This is in agreement with data showing sta-  
 949 ble levels of C83 in the frontal cortex of 5xFAD mice  
 950 lacking MT5-MMP [17]. Unlike CTF modulation,  
 951 MT5-MMP deficiency resulted in a decrease of A $\beta$   
 952 levels, which could not be correlated with increases in  
 953 A $\beta$ -degrading enzymes. In fact, the observed reduc-  
 954 tion in neprilysin (*Mme*) is somewhat counterintuitive,  
 955 unless it actually underlies a negative feedback response  
 956 to a potential increase in neprilysin activity. Analysis of  
 957 genes involved in A $\beta$  transport/clearance (e.g., *Lrp1*,  
 958 *Lrp8*, *Ldlr*, *Ager*) also revealed no clear evidence of a  
 959 transcriptional mechanism that could explain the mod-  
 960 ulation of A $\beta$  content.

### 961 MT5-MMP deficiency prevents the accumulation 962 of overexpressed C99 and hence A $\beta$

963 The above data denote the capacity of MT5-MMP to con-  
 964 trol A $\beta$  levels, echoing our pioneer work in vivo [13], and  
 965 demonstrate that functional interactions of MT5-MMP  
 966 with APP/A $\beta$  may already happen in developing neural  
 967 cells. However, the inability to detect C99 in these cells  
 968 led us to question whether MT5-MMP might also con-  
 969 trol C99 as it does in adult mice [13, 17]. We answered  
 970 this doubt by providing evidence that the levels of trans-  
 971 duced human C99 were downregulated in MT5-MMP-  
 972 deficient primary neurons and, therefore, also those of  
 973 A $\beta$ . It is noteworthy that C83 derived from overexpressed  
 974 C99 was also downregulated in MT5-MMP-deficient  
 975 neurons, in contrast to the lack of effect on constitutive  
 976 C83 likely resulting from APP processing. Thus, the con-  
 977 trol of C83 by MT5-MMP seems to depend mostly on  
 978 whether it is generated from APP or C99. Taken together,  
 979 these data indicate that young neurons have the poten-  
 980 tial to prevent the accumulation of endogenous C99 and  
 981 thus prevent the derived detrimental consequences. They  
 982 also highlight that MT5-MMP deficiency facilitates C99  
 983 degradation in these neurons, which supports our recent  
 984 results in HEK cells showing that deletion of C-terminal



985 domains of MT5-MMP does indeed lead to C99 degra-  
986 tion [32].

987 **Concluding remarks**

988 The present work unveils regulatory events in develop-  
989 ing neural cells that may influence early AD pathogen-  
990 esis through functional interactions between MT5-MMP  
991 and IL-1β. It is noteworthy that inflammation and neu-  
992 ronal activity are particularly regulated by AD genotype  
993 and MT5-MMP in young cells, suggesting that they are  
994 important early markers of pathology onset in an AD  
995 settings. Similarly, IL-1β appears to be a selective mod-  
996 ulator of neuroinflammation and neuronal activity in  
997 these young cells, although the complexity of the effects  
998 (or lack thereof) of the cytokine must take into account  
999 the limitations of our experimental setting, which does  
1000 not preclude, for example, different results at different  
1001 cytokine concentrations. Overall, MT5-MMP appears to  
1002 be a multifaceted modulator at the cross roads of neuro-  
1003 inflammation, APP metabolism, and synaptic function,  
1004 further enhancing interest in this proteinase and the pos-  
1005 sible therapeutic implications of its modulation in AD.

1007 **Abbreviations**

1008 3xTG: Transgenic mice expressing human APP MAPT and PSEN1 genes with 3  
1009 familial mutations; 5xFAD: Transgenic mice expressing human APP and PSEN1  
1010 genes with 5 familial mutations; AAV: Adeno-associated virus; A.U.: Arbitrary  
1011 units; AD: Alzheimer's disease; Aβ: Amyloid β peptide; ACE: Angiotensin  
1012 converting enzyme; ADAM10: A Disintegrin And Metalloproteinase 10;  
1013 APP: Amyloid precursor protein; BACE1: Beta-site APP cleaving enzyme 1  
1014 (β-secretase); C99/C83: APP CTF of 99/83 amino acids; CTF: C-terminal frag-  
1015 ment; DAPT: N-[N-(3,5-difluorophenacetyl)-L-alanyl]-S-phenylglycine t-butyl  
1016 ester, γ-Secretase inhibitor; DIV: Days in vitro; FL: Full length; ICC: Immunocy-  
1017 tochemistry; ECE: Endothelin converting enzyme; IB: Immunoblot; IDE: Insulin  
1018 degrading enzyme; IL-1β/6: Interleukin-1β/6; LDLR: Low-density lipoprotein  
1019 receptor; LRP1/8: Low-density lipoprotein related-protein 1/8; LTP: Long-term  
1020 potentiation; MCP-1: Monocyte chemoattractant protein-1 (Ccl2); MG132:  
1021 Proteasome inhibitor; MMP-2/-9: Matrix metalloproteinase; MT1/5-MMP:  
1022 Membrane-type 1/5-matrix metalloproteinase; O.D.: Optical density; PSEN1:  
1023 Presenilin 1; RAGE: Receptor for advanced aged products; RT-qPCR: Reverse  
1024 transcription-quantitative PCR; sAPP95: Soluble amyloid protein precursor  
1025 fragment generated by MT5-MMP; sAPPα/β: Soluble APPα/β; sAPPFL: Full  
1026 length soluble amyloid protein precursor; TTX: Tetrodotoxin; WB: Western blot;  
1027 WT: Wild type.

1028 **Supplementary Information**

1029 The online version contains supplementary material available at <https://doi.org/10.1186/s12974-022-02407-z>.

1031 **Additional file 1.** A Measurement of human A levels (pg/mL) in Tg and  
1032 TgMT5-/- cultures using the ThermoFisher Scientific ELISA kit. B and C.  
1033 mRNA levels of hAPP and hPSEN1 analyzed by RT-qPCR in Tg and TgMT5-/-  
1034 cultures and normalized with Gapdh as housekeeping gene. Black bars  
1035 represent control (untreated) conditions and grey bars IL-1β treated con-  
1036 ditions (10 ng/mL for 24 h). Values are the mean ± SEM of 3–5 independ-  
1037 ent cultures by genotype.

1038 **Additional file 2.** Immunoblots representing subcellular distribution of  
1039 C83 detected with the APP-CTF antibody in primary cortical cultures at  
1040 11 DIV. Fractions are represented with their loading controls: for fraction

1, cytosolic—GAPDH; for fraction 2, membranous—Na + /K + ATPase,  
and for fraction 3, nuclear—Histone 3. Cells were treated or not with  
DAPT (10 μM). AAV-C99 (right) indicates a positive control. WT cells were  
infected for 5 days with AAV-C99 and recovered at 11 DIV. Note that only  
C83 levels were detectable with DAPT treatment.

1041  
1042  
1043  
1044  
1045

**Acknowledgements**

We thank Eliane Charrat for the technical assistance and Dr. Frédéric Checler and Dr. Raphaëlle Pardossi-Piquard for sharing the AVV-C99 constructs.

1046  
1047  
1048

**Authors' contributions**

DP, JMP, LGG, LL, DS, CM and KB performed experiments other than electro-physiology. ED designed, performed and analyzed electrophysiological exper-iments. MK contributed to the experimental design. KB and SR designed the experiments, analyzed data, supervised the project and wrote the paper. All authors discussed the results and reviewed the manuscript. All authors read and approved the final manuscript.

1049  
1050  
1051  
1052  
1053  
1054  
1055

**AQ1**

**Funding**

This work was supported by funding from the CNRS and Aix-Marseille Université and by public grants overseen by the French National Research Agency (ANR), MAD5 to SR, as part of the second "Investissements d'Avenir" program. The work was also supported by the DHUNE center of excellence and a CoEN (ADMIRE-MT5) grant to SR, by the Fondation pour la Recherche Médicale (FRM) and Fondation Alzheimer (ALZ201912009627) to SR, and by Fondation Vaincre l'Alzheimer grants to SR. DP received support from the French government under the Programme Investissements d'Avenir, Initiative d'Excellence d'Aix-Marseille Université via A\*Mixex (AMX-19-IET-004) and ANR (ANR-17-EURE-0029) funding. DP was also a recipient of FRM fund- ing—FDT202001011017. JMP was recipient of a doctoral fellowship from Fondation Vaincre l'Alzheimer. LGG was granted by the ANR and by the FRM FDT201904008423 fellowshp. KB was granted a research associate fellowship (Management of Talents) by Excellence Initiative of Aix-Marseille University-A\*MIDEX, a French "Investissements d'Avenir".

1056  
1057  
1058  
1059  
1060  
1061  
1062  
1063  
1064  
1065  
1066  
1067  
1068  
1069  
1070  
1071

**Availability of data and materials**

All data generated or analyzed during this study are included in this published article and are available from the corresponding author on reasonable request.

1072  
1073  
1074  
1075

**Declarations**

All data generated or analyzed during this study are included in this published article and are available from the corresponding author on reasonable request.

**Ethics approval and consent to participate**

All these experimental procedures were conducted in accordance with National and European regulations (EU directive N° 2010/63), and in agree- ment with the authorization for animal experimentation attributed to the laboratory (research project: APAFIS#23040-2019112708474721 v4).

1077  
1078  
1079  
1080  
1081

**Consent for publication**

Not applicable.

1082  
1083

**Competing interests**

The authors declare no financial conflict of interest that might be construed to influence the results or interpretation of the manuscript.

1084  
1085  
1086

**Author details**

<sup>1</sup>Institute of Neuropathophysiology (INP), UMR 7051, Aix-Marseille Univ, CNRS, Campus Santé Timone, 27 Bld Jean Moulin, 13005 Marseille, France. <sup>2</sup>Present Address: Department of Neurology, Northwestern University Feinberg School of Medicine, Chicago, IL, USA. <sup>3</sup>Present Address: BarcelonaBeta Brain Research Center (BBRC), Pasqual Maragall Foundation, Barcelona, Spain.

1087  
1088  
1089  
1090  
1091  
1092

Received: 19 July 2021 Accepted: 30 January 2022

1093  
1094



## References

- 1095  
1096  
1097  
1098  
1099  
1100  
1101  
1102  
1103  
1104  
1105  
1106  
1107  
1108  
1109  
1110  
1111  
1112  
1113  
1114  
1115  
1116  
1117  
1118  
1119  
1120  
1121  
1122  
1123  
1124  
1125  
1126  
1127  
1128  
1129  
1130  
1131  
1132  
1133  
1134  
1135  
1136  
1137  
1138  
1139  
1140  
1141  
1142  
1143  
1144  
1145  
1146  
1147  
1148  
1149  
1150  
1151  
1152  
1153  
1154  
1155  
1156  
1157  
1158  
1159  
1160  
1161  
1162  
1163  
1164
1. Rivera S, García-González L, Khrestchatsky M, Baranger K. Metalloproteinases and their tissue inhibitors in Alzheimer's disease and other neurodegenerative disorders. *Cell Mol Life Sci*. 2019;76(16):3167–91.
  2. Jaworski DM. Developmental regulation of membrane type-5 matrix metalloproteinase (MT5-MMP) expression in the rat nervous system. *Brain res*. 2000;860(1–2):174–7.
  3. Rivera S, Khrestchatsky M, Kaczmarek L, Rosenberg GA, Jaworski DM. Metzincin proteases and their inhibitors: foes or friends in nervous system physiology? *J Neurosci*. 2010;30(46):15337–57.
  4. García-González L, Pilát D, Baranger K, Rivera S. Emerging alternative proteinases in APP metabolism and Alzheimer's Disease pathogenesis: a focus on MT1-MMP and MT5-MMP. *Front Aging Neurosci*. 2019;11:244.
  5. Hayashita-Kinoh H, Kinoh H, Okada A, Komori K, Itoh Y, Chiba T, et al. Membrane-type 5 matrix metalloproteinase is expressed in differentiated neurons and regulates axonal growth. *Cell Growth Differ*. 2001;12:573–80.
  6. Komori K, Nonaka T, Okada A, Kinoh H, Hayashita-Kinoh H, Yoshida N, et al. Absence of mechanical allodynia and  $\beta$ -fiber sprouting after sciatic nerve injury in mice lacking membrane-type 5 matrix metalloproteinase. *FEBS Lett*. 2004;557(1–3):125–8.
  7. Porlan E, Martí-Prado B, Morante-Redolat JM, Consiglio A, Delgado AC, Kypta R, et al. MT5-MMP regulates adult neural stem cell functional quiescence through the cleavage of N-cadherin. *Nat Cell Biol*. 2014;16(7):629–38.
  8. Monea S, Jordan BA, Srivastava S, DeSouza S, Ziff EB. Membrane localization of membrane type 5 matrix metalloproteinase by AMPA receptor binding protein and cleavage of cadherins. *J Neurosci*. 2006;26:2300–12.
  9. Restituto S, Khatri L, Ninan I, Mathews PM, Liu X, Weinberg RJ, et al. Synaptic autoregulation by metalloproteinases and  $\gamma$ -secretase. *J Neurosci*. 2011;31:12083–93.
  10. Folgueras AR, Valdes-Sanchez T, Llano E, Menendez L, Baamonde A, Denlinger BL, et al. Metalloproteinase MT5-MMP is an essential modulator of neuro-immune interactions in thermal pain stimulation. *Proc Natl Acad Sci*. 2009;106(38):16451–6.
  11. Ahmad M, Takino T, Miyamori H, Yoshizaki T, Furukawa M, Sato H. Cleavage of amyloid-beta precursor protein (APP) by membrane-type matrix metalloproteinases. *J Biochem*. 2006;139(3):517–26.
  12. Willem M, Tahirovic S, Busche MA, Ovsepian SV, Chafai M, Kootar S, et al.  $\eta$ -Secretase processing of APP inhibits neuronal activity in the hippocampus. *Nature*. 2015;526(7573):443–7.
  13. Baranger K, Marchalant Y, Bonnet AE, Crouzin N, Carrete A, Paumier J-M, et al. MT5-MMP is a new pro-amyloidogenic proteinase that promotes amyloid pathology and cognitive decline in a transgenic mouse model of Alzheimer's disease. *Cell Mol Life Sci*. 2016;73(1):217–36.
  14. Selkoe DJ, Hardy J. The amyloid hypothesis of Alzheimer's disease at 25 years. *EMBO Mol Med*. 2016;8(6):595–608.
  15. Woodruff G, Reyna SM, Dunlap M, Van Der Kant R, Callender JA, Young JE, et al. Defective transcytosis of APP and lipoproteins in human iPSC-derived neurons with familial Alzheimer's disease mutations. *Cell Rep*. 2016;17(3):759–73.
  16. Tan JZA, Gleeson PA. The trans-Golgi network is a major site for alpha-secretase processing of amyloid precursor protein in primary neurons. *J Biol Chem*. 2019;294(5):1618–31.
  17. Baranger K, Bonnet AE, Girard SD, Paumier J-M, García-González L, Elmanaa W, et al. MT5-MMP Promotes Alzheimer's Pathogenesis in the Frontal Cortex of 5xFAD Mice and APP Trafficking in vitro. *Front Mol Neurosci*. 2017;9.
  18. Heneka MT, Golenbock DT, Latz E. Innate immunity in Alzheimer's disease. *Nat Immunol*. 2015;16(3):229–36.
  19. Freeman LC, Ting JP-Y. The pathogenic role of the inflammasome in neurodegenerative diseases. *J Neurochem*. 2016;136:29–38.
  20. Heneka MT, McManus RM, Latz E. Inflammasome signalling in brain function and neurodegenerative disease. *Nat Rev Neurosci*. 2018;19(10):610–21.
  21. Tong L, Prieto GA, Kramar EA, Smith ED, Cribbs DH, Lynch G, et al. Brain-derived neurotrophic factor-dependent synaptic plasticity is suppressed by interleukin-1 via p38 mitogen-activated protein kinase. *J Neurosci*. 2012;32(49):17714–24.
  22. Viviani B, Gardoni F, Bartesaghi S, Corsini E, Facchi A, Galli CL, et al. Interleukin-1 $\beta$  released by gp120 drives neural death through tyrosine phosphorylation and trafficking of NMDA receptors. *J Biol Chem*. 2006;281(40):30212–22.
  23. Mishra A, Kim HJ, Shin AH, Thayer SA. Synapse loss induced by interleukin-1 $\beta$  requires pre- and post-synaptic mechanisms. *J Neuroimmune Pharmacol*. 2012;7(3):571–8.
  24. Domingues C, da Cruz e Silva OAB, Henriques AG. Impact of Cytokines and Chemokines on Alzheimer's Disease Neuropathological Hallmarks. *Curr Alzheimer Res*. 2017;14(8).
  25. Tachida Y, Nakagawa K, Saito T, Saido TC, Honda T, Saito Y, et al. Interleukin-1 $\beta$  up-regulates TACE to enhance  $\alpha$ -cleavage of APP in neurons: resulting decrease in A $\beta$  production. *J Neurochem*. 2008;104(5):1387–93.
  26. Shaftel SS, Kyrkanides S, Olschowka JA, Miller JH, Johnson RE, O'Banion MK. Sustained hippocampal IL-1 $\beta$  overexpression mediates chronic neuroinflammation and ameliorates Alzheimer plaque pathology. *J Clin Invest*. 2007;117(6):1595–604.
  27. Rivera-Escalera F, Pinney JJ, Owlett L, Ahmed H, Thakar J, Olschowka JA, et al. IL-1 $\beta$ -driven amyloid plaque clearance is associated with an expansion of transcriptionally reprogrammed microglia. *J Neuroinflammation*. 2019;16(1):261.
  28. Baranger K, Khrestchatsky M, Rivera S. MT5-MMP; just a new APP processing proteinase in Alzheimer's disease? *J Neuroinflammation*. 2016;13(1):167.
  29. Lauritzen I, Pardossi-Piquard R, Bourgeois A, Pagnotta S, Biferi MG, Barkats M, et al. Intraneuronal aggregation of the beta-CTF fragment of APP (C99) induces Abeta-independent lysosomal-autophagic pathology. *Acta Neuropathol*. 2016;132(2):257–76.
  30. Gilda JE, Gomes AV. Stain-Free total protein staining is a superior loading control to  $\beta$ -actin for Western blots. *Anal Biochem*. 2013;440(2):186–8.
  31. Sander H, Wallace S, Plouse R, Tiwari S, Gomes AV. Ponceau S waste: Ponceau S staining for total protein normalization. *Anal Biochem*. 2019;575:44–53.
  32. García-González L, Paumier J, Louis L, Pilát D, Bernard A, Stephan D, et al. MT5-MMP controls APP and  $\beta$ -CTF/C99 metabolism through proteolytic-dependent and -independent mechanisms relevant for Alzheimer's disease. *FASEB J*. 2021;35(7).
  33. Paumier J-M, Py NA, García-González L, Bernard A, Stephan D, Louis L, et al. Proamyloidogenic effects of membrane type 1 matrix metalloproteinase involve MMP-2 and BACE-1 activities, and the modulation of APP trafficking. *FASEB J*. 2019;33(2):2910–27.
  34. Py NA, Bonnet AE, Bernard A, Marchalant Y, Charrat E, Checler F, et al. Differential spatio-temporal regulation of MMPs in the 5xFAD mouse model of Alzheimer's disease: evidence for a pro-amyloidogenic role of MT1-MMP. *Front Aging Neurosci*. 2014;6.
  35. Cahill CM, Rogers JT. Interleukin (IL) 1 $\beta$  induction of IL-6 is mediated by a novel phosphatidylinositol 3-kinase-dependent AKT/I $\kappa$ B kinase  $\alpha$  pathway targeting activator protein-1. *J Biol Chem*. 2008;283(38):25900–12.
  36. Lu Y, Jiang B-C, Cao D-L, Zhang Z-J, Zhang X, Ji R-R, et al. TRAF6 upregulation in spinal astrocytes maintains neuropathic pain by integrating TNF- $\alpha$  and IL-1 $\beta$  signaling. *Pain*. 2014;155(12):2618–29.
  37. Basu A, Krady JK, O'Malley M, Styren SD, DeKosky ST, Levison SW. The type 1 interleukin-1 receptor is essential for the efficient activation of microglia and the induction of multiple proinflammatory mediators in response to brain injury. *J Neurosci*. 2002;22(14):6071–82.
  38. Allan SM, Tyrrell PJ, Rothwell NJ. Interleukin-1 and neuronal injury. *Nat Rev Immunol*. 2005;5(8):629–40.
  39. Ng A, Tam WW, Zhang MW, Ho CS, Husain SF, McIntyre RS, et al. IL-1 $\beta$ , IL-6, TNF- $\alpha$  and CRP in elderly patients with depression or Alzheimer's disease: systematic review and meta-analysis. *Sci Rep*. 2018;8(1):12050.
  40. Kaur D, Sharma V, Deshmukh R. Activation of microglia and astrocytes: a roadway to neuroinflammation and Alzheimer's disease. *Inflammopharmacology*. 2019;27(4):663–77.
  41. Schönbeck U, Mach F, Libby P. Generation of biologically active IL-1 beta by matrix metalloproteinases: a novel caspase-1-independent pathway of IL-1 beta processing. *J Immunol*. 1998;161(7):3340–6.
  42. Charlesworth P, Cotterill E, Morton A, Grant S, Eglan SJ. Quantitative differences in developmental profiles of spontaneous activity in cortical and hippocampal cultures. *Neural Dev*. 2015;10(1):1.
  43. Giovannini MG, Scali C, Prosperi C, Bellucci A, Vannucchi MG, Rosi S, et al. Beta-amyloid-induced inflammation and cholinergic hypofunction in the



- 1235 rat brain in vivo: involvement of the p38MAPK pathway. *Neurobiol Dis.* 2002;11(2):257–74.
- 1236
- 1237 44. Gasic-Milenkovic J, Dukic-Stefanovic S, Deuther-Conrad W, Gärtner U, Münch G. Beta-amyloid peptide potentiates inflammatory responses induced by lipopolysaccharide, interferon- $\gamma$  and « advanced glycation endproducts » in a murine microglia cell line. *Eur J Neurosci.* 2003;17(4):813–21.
- 1238
- 1239 45. Lauritzen I, Pardossi-Piquard R, Bauer C, Brigham E, Abraham JD, Rinaldi S, et al. The beta-secretase-derived C-terminal fragment of betaAPP, C99, but not Abeta, is a key contributor to early intraneuronal lesions in triple-transgenic mouse hippocampus. *J Neurosci.* 2012;32(46):16243–55.
- 1240
- 1241 46. Sennvik K, Boekhoorn K, Lasrado R, Terwel D, Verhaeghe S, Korh H, et al. Tau-4R suppresses proliferation and promotes neuronal differentiation in the hippocampus of tau knockin/ knockout mice. *FASEB J.* 2007;21(9):2149–61.
- 1242
- 1243 47. Storck SE, Meister S, Nahrath J, Meißner JN, Schubert N, Di Spiezio A, et al. Endothelial LRP1 transports amyloid- $\beta$ 1–42 across the blood-brain barrier. *J Clin Invest.* 2015;126(1):123–36.
- 1244
- 1245 48. Liu C-C, Hu J, Zhao N, Wang J, Wang N, Cirrito JR, et al. Astrocytic LRP1 mediates brain A $\beta$  clearance and impacts amyloid deposition. *J Neurosci.* 2017;37(15):4023–31.
- 1246
- 1247 49. Shinohara M, Tachibana M, Kanekiyo T, Bu G. Role of LRP1 in the pathogenesis of Alzheimer's disease: evidence from clinical and preclinical studies. *J Lipid Res.* 2017;58(7):1267–81.
- 1248
- 1249 50. Van Gool B, Storck SE, Reekmans SM, Lechat B, Gordts PLSM, Pradier L, et al. LRP1 has a predominant role in production over clearance of A $\beta$  in a mouse model of Alzheimer's disease. *Mol Neurobiol.* 2019;56(10):7234–45.
- 1250
- 1251 51. Fuentealba RA, Barría M, Lee J, Cam J, Araya C, Escudero CA, et al. ApoER2 expression increases A $\beta$  production while decreasing Amyloid Precursor Protein (APP) endocytosis: possible role in the partitioning of APP into lipid rafts and in the regulation of  $\gamma$ -secretase activity. *Mol Neurodegener.* 2007;2(1):14.
- 1252
- 1253 52. Katsouri L, Georgopoulos S. Lack of LDL receptor enhances amyloid deposition and decreases glial response in an Alzheimer's Disease mouse model. *PLoS ONE.* 2011;6(7):e21880.
- 1254
- 1255 53. Fang F, Yu Q, Arancio O, Chen D, Gore SS, Yan SS, et al. RAGE mediates A $\beta$  accumulation in a mouse model of Alzheimer's disease via modulation of  $\beta$ - and  $\gamma$ -secretase activity. *Hum Mol Genet.* 2018;27(6):1002–14.
- 1256
- 1257 54. Llorente P, Martins S, Sastre I, Aldudo J, Recuero M, Adjaye J, et al. Matrix metalloproteinase 14 mediates APP proteolysis and lysosomal alterations induced by oxidative stress in human neuronal cells. *Ox Med Cell Longev.* 2020;2020:1–13.
- 1258
- 1259 55. Hernandez-Guillamon M, Mawhirt S, Blais S, Montaner J, Neubert TA, Rostagno A, et al. Sequential amyloid- $\beta$  degradation by the matrix metalloproteases MMP-2 and MMP-9. *J Biol Chem.* 2015;290(24):15078–91.
- 1260
- 1261 56. Song M-S, Learman CR, Ahn K-C, Baker GB, Kippe J, Field EM, et al. In vitro validation of effects of BDNF-expressing mesenchymal stem cells on neurodegeneration in primary cultured neurons of APP/PS1 mice. *Neuroscience.* 2015;307:37–50.
- 1262
- 1263 57. Thornton P, Pinteaux E, Gibson RM, Allan SM, Rothwell NJ. Interleukin-1-induced neurotoxicity is mediated by glia and requires caspase activation and free radical release. *J Neurochem.* 2006;98(1):258–66.
- 1264
- 1265 58. Corbett GT, Roy A, Pahan K. Gemfibrozil, a lipid-lowering drug, upregulates IL-1 receptor antagonist in mouse cortical neurons: implications for neuronal self-defense. *J Immunol.* 2012;189(2):1002–13.
- 1266
- 1267 59. van Gijssel-Bonnello M, Baranger K, Benech P, Rivera S, Khrestchatsky M, de Reggi M, et al. Metabolic changes and inflammation in cultured astrocytes from the 5xFAD mouse model of Alzheimer's disease: alleviation by pantethine. *PLoS ONE.* 2017;12(4):e0175369.
- 1268
- 1269 60. François A, Terro F, Janet T, Bilan AR, Paccalin M, Page G. Involvement of interleukin-1 $\beta$  in the autophagic process of microglia: relevance to Alzheimer's disease. *J Neuroinflammation.* 2013;10(1):915.
- 1270
- 1271 61. Francois A, Terro F, Quellard N, Fernandez B, Chassaing D, Janet T, et al. Impairment of autophagy in the central nervous system during lipopolysaccharide-induced inflammatory stress in mice. *Mol Brain.* 2014;7(1):56.
- 1272
- 1273 62. Zott B, Busche MA, Sperling RA, Konnerth A. What happens with the circuit in Alzheimer's disease in mice and humans? *Annu Rev Neurosci.* 2018;41:277–97.
- 1274
- 1275 63. Vezzani A, Viviani B. Neuromodulatory properties of inflammatory cytokines and their impact on neuronal excitability. *Neuropharmacology.* 2015;96:70–82.
- 1276
- 1277 64. Viviani B, Bartesaghi S, Gardoni F, Vezzani A, Behrens MM, Bartfai T, et al. Interleukin-beta enhances NMDA receptor-mediated intracellular calcium increase through activation of the Src family of kinases. *J Neurosci.* 2003;23:8692–700.
- 1278
- 1279 65. Wang S, Cheng Q, Malik S, Yang J. Interleukin-1beta inhibits gamma-aminobutyric acid type A (GABA(A)) receptor current in cultured hippocampal neurons. *J Pharmacol Exp Ther.* 2000;292(2):497–504.
- 1280
- 1281 66. De Chiara V, Motta C, Rossi S, Studer V, Barbieri F, Lauro D, et al. Interleukin-1 $\beta$  alters the sensitivity of cannabinoid CB1 receptors controlling glutamate transmission in the striatum. *Neuroscience.* 2013;250:232–9.
- 1282
- 1283 67. Siwek ME, Müller R, Henseler C, Trog A, Lundt A, Wormuth C, et al. Altered theta oscillations and aberrant cortical excitatory activity in the 5XFAD model of Alzheimer's disease. *Neural Plast.* 2015;2015:781731.
- 1284
- 1285 68. Sompol P, Furman JL, Pleiss MM, Kraner SD, Artiushin IA, Batten SR, et al. Calcineurin/NFAT signaling in activated astrocytes drives network hyperexcitability in A $\beta$ -bearing mice. *J Neurosci.* 2017;37(25):6132–48.
- 1286
- 1287 69. Lai AY, Swayze RD, El-Husseini A, Song C. Interleukin-1 beta modulates AMPA receptor expression and phosphorylation in hippocampal neurons. *J Neuroimmunol.* 2006;175(1–2):97–106.
- 1288
- 1289 70. Murray C. Interleukin-1beta inhibits glutamate release in hippocampus of young, but not aged, Rats. *Neurobiol Aging.* 1997;18(3):343–8.
- 1290
- 1291 71. Vereker E, O'Donnell E, Lynch MA. The inhibitory effect of interleukin-1 $\beta$  on long-term potentiation is coupled with increased activity of stress-activated protein kinases. *J Neurosci.* 2000;20(18):6811–9.
- 1292
- 1293 72. Cebo C, Dambrouck T, Maes E, Laden C, Strecker G, Michalski J-C, et al. Recombinant human interleukins IL-1 $\alpha$ , IL-1 $\beta$ , IL-4, IL-6, and IL-7 show different and specific calcium-independent carbohydrate-binding properties. *J Biol Chem.* 2001;276(8):5685–91.
- 1294
- 1295 73. Rice HC, de Malmazet D, Schreurs A, Frere S, Van Molle I, Volkov AN, et al. Secreted amyloid-beta precursor protein functions as a GABABR1a ligand to modulate synaptic transmission. *Science.* 2019;363(6423).
- 1296
- 1297 74. Lauritzen I, Becot A, Bourgeois A, Pardossi-Piquard R, Biferi MG, Barkats M, et al. Targeting gamma-secretase triggers the selective enrichment of oligomeric APP-CTFs in brain extracellular vesicles from Alzheimer cell and mouse models. *Trans Neurodegener.* 2019;8:35.
- 1298
- 1299 75. Vaillant-Beuchot L, Mary A, Pardossi-Piquard R, Bourgeois A, Lauritzen I, Eysert F, et al. Accumulation of amyloid precursor protein C-terminal fragments triggers mitochondrial structure, function, and mitophagy defects in Alzheimer's disease models and human brains. *Acta Neuropathol.* 2021;141(1):39–65.
- 1300
- 1301
- 1302
- 1303

## Publisher's Note

Springer Nature remains neutral with regard to jurisdictional claims in published maps and institutional affiliations.

Ready to submit your research? Choose BMC and benefit from:

- fast, convenient online submission
- thorough peer review by experienced researchers in your field
- rapid publication on acceptance
- support for research data, including large and complex data types
- gold Open Access which fosters wider collaboration and increased citations
- maximum visibility for your research: over 100M website views per year

At BMC, research is always in progress.

Learn more [biomedcentral.com/submissions](https://biomedcentral.com/submissions)



Journal : **BMCTwo 12974**

Article No : **2407**

MS Code :

Dispatch : **3-2-2022**

LE

CP

Pages : **21**

TYPESET

DISK